FIELD-OF-VIEW DETERMINATION FOR A BINDWEED DETECTION SENSOR

By

BYRON RAY CRINER

Bachelor of Science

Oklahoma State University

Stillwater, Oklahoma

1994

Submitted to the Faculty of the
Graduate College of the
Oklahoma State University
in partial fulfillment of
the requirements for
the Degree of
MASTER OF SCIENCE
May, 1998

FIELD-OF-VIEW DETERMINATION FOR A

BINDWEED DETECTION SENSOR

Thesis Approved:

John B. Solie

Thesis Adviser

Marvin Stone

Richard W. Whitney

Wayne B. Powell

Dean of the Graduate College

ACKNOWLEDGMENTS

I would like to tank my major advisor, Dr. John B. Solie, and my committee members, Dr. Richard W. Whitney and Dr. Marvin L Stone, for their guidance, suggestions, and insight throughout this research project and my time at Oklahoma State University. Their knowledge, experience, and positive attitude have been an invaluable part of my professional development. Additionally, I would like to acknowledge the graduate and undergraduate students who worked on this project, who without, I would have never completed.

I would like to give very special thanks to my family for their never ending support and devotion, especially my wife, Tania. She has been my source of strength, my constant companion, and my greatest inspiration throughout the entire process.

TABLE OF CONTENTS

Chapter — Page

I. Introduction 1

II. Simulation to Determine Field-of-view for a Bindweed Detection Sensor 2

Abstract 2
Introduction 3
Methods 7
Simulation 10
Results and Discussion 15
Conclusion 23
References 24

III. Field-of-view Determination for a Bindweed Detection Sensor 27

Abstract 27
Introduction 28
Methods 32
Results and Discussion 41
Conclusion 47
References 50

IV. Recommendations for Further Study 53

Appendix Visual Basic Programs Used in Chapters II and III 55

LIST OF TABLES

Table Page

Chapter II

1. Error equation coefficients 20
2. Bindweed Simulation Results.. 21

Chapter III

1. Results of paired t-test and sample set detection error 43
2. Error equation coefficients 49
3. NDVI threshold and threshold error for all unpaired analysis 46

LIST OF FIGURES

Figure Page

Chapter II

1. Lawn tractor field collection apparatus 8
2. Simulation process to select RED and NIR values of a single pixel 11
3. Threshold selection and error determination from simulation for a sensor field-of-view 14
4. Typical reflectance curves for bindweed and soil from study field 15
5. 9/11/96—Error verses percent of field-of-view covered by bindweed 16
6. 9/23/96—Error verses percent of field-of-view covered by bindweed 17
7. 10/2/96 Clear—Error verses percent of field-of-view covered by bindweed..... 17
8. 10/2/96 Shadow—Error verses percent of field-of-view covered by bindweed 18
9. 10/25/96 Clear—Error verses percent of field-of-view covered by bindweed 18
10. 10/25/96 Shadow—Error verses percent of field-of-view covered by bindweed 19
11. 10/31/96—Error verses percent of field-of-view covered by bindweed 19

Chapter III

1. Photoelectric diode sensor 35
2. Sensor Response Curves for Sensor Image Size Determination 36
3. Sensor mounted on angle frame 36
4. Layout of field transect 37
5. Creation of fields-of-view by adding contiguous 0.065 m^2 sensor readings 39
6. Typical sensor response; with and without bindweed for 11 fields-of-view. Transects from 10/2/97 and 10/15/97 42
7. Errors vs. NDVI threshold from unpaired analysis. Error curves for 0.065, 0.129, and 0.194 m^2 fields-of-view 44
8. Threshold error vs. field-of-view size 45

Chapter I

Introduction

This thesis is composed of two manuscripts formatted for submission to the American Society of Agricultural Engineers and a final chapter with recommendations of additional study in this area. Chapter II, "Simulation to determine field-of-view for a bindweed detection sensor" and Chapter III, "Field-of-view determination for a bindweed detection sensor", are complete as written and do not require any additional support material. Both manuscripts are original research by the author under advisement by Dr. J. B. Solie, PE, Dr. R. W. Whitney, PE, and Dr. M. L. Stone.

Chapter II

Simulation to Determine Field-of-view for a Bindweed Detection Sensor

Abstract

One alternative to uniform herbicide application is to selectively spray only the weeds in a field. The objective of this research was to use a sensor simulation, based on spectrometer data from bindweed, *Convolvulus arvensis* and soil to determine the maximum required sensor field-of-view by which NDVI can be reliably used to detect a target bindweed on bare soil. Reflected electromagnetic energy from 2030 mm^2 bindweed and soil areas was measured with a spectrometer as inputs for a sensor simulation program. The program used red (670 nm) and near-infrared (780 nm) irradiance to simulate the use of multiple sensors each with a different field-of-view, collecting random field samples under seven different sets of environmental conditions. No single field-of-view size was optimum for all sets of test conditions. Results of the simulations were expressed as error versus the percentage of field-of-view that must be covered by bindweed to insure detection. The median required weed cover for all data was 0.79% of the field-of-view with 10% error and 1.48% with 5% error. To detect a target bindweed of 6090 mm^2, these correspond to fields-of-view of 0.77 m^2 and 0.41 m^2, respectively. The maximum required bindweed cover for any test condition at 10% error was 7.78%, and the minimum was 0.04%. Variability in sensor measurements was due to

differences in reflective properties of bindweed and soil, and variations in the sunlight striking these targets.

Keywords: Simulation, sensor, weed, detection

Introduction

Every year farmers throughout the world spend millions of dollars on tillage and herbicide in an attempt to control undesirable weed species in crop fields. In much of the United States, one of the most serious and difficult weed problems is field bindweed, *Convolvulus arvensis* (Field bindweed, *Convolvulus arvensis,* 1998). Bindweed is a member of the Morning-glory family and has multiple lateral runners, a long taproot, and arrow shaped leaves. Dense infestations of field bindweed may reduce crop yields by 50 to 60% (Zollinger, 1996). Tillage is the most widely accepted method of control, but to effectively control bindweed requires months of regular tillage operations (Majek, 1993). Occasional tillage may in fact help spread the weed and make problems worse.

The alternative to tillage weed control is chemical herbicides. Currently chemical herbicides are applied uniformly across an entire field which may have only a sparse or patchy population of weeds. To insure weed control, large amounts of chemical are applied, much of which falls on weed-free areas and will never reach the target plant. A large percentage of the herbicide and, consequently, the farmer's money is wasted. This waste of herbicide has a very real and negative effect on the profitability of crop production, as well as a potentially adverse environmental impact.

In an era of increasing operating costs, heightened awareness of environmental impact, and escalating regulation of agri-chemicals, a more efficient and environmentally conscious method of herbicide application is needed. One alternative to the usual method of uniform application is to selectively spray only the weeds in a field. With improving technology, it may now be possible to detect and spray weeds on the go using remote sensors and intermittent chemical applicators. A site specific herbicide system would utilize remote sensed data from either on-board sensors or overhead imagery to develop a vegetative index (VI) for small areas, or elements, of a field. Based on the index, the system would then make a decision of the presence or absence of a weed in each field element. This decision would be translated to a spray command and carried out by computer controlled applicators.

Bindweed control in winter wheat is a prime application for such technology. Bindweed can be treated in late summer or early fall, when winter wheat fields are fallow, and it can be reliably assumed that any growing plants are weeds. The task of the sensor and controller is then simply sense and distinguish what is plant and should be sprayed from what is soil and should not.

A number of systems sensing electromagnetic energy have been developed in an attempt to detect and selectively spray weeds. Stone (1994) used an optical sensor and an artificial neural network to detect bindweed. This sensor measured reflected energy in three bands: green, red, and near-infrared (NIR). This unit was able to detect 92% of the cases where weeds were present and reject 80% of the cases where weeds were not present. Felton et al. (1991) developed a spray system with remote sensors that also used reflected energy in the red and near-infrared wavebands as a means of distinguishing between plants and soil. He estimated the mean reduction in area sprayed was 90%. Beck (1996) reported on a second selective sprayer that used silicon PIN photodetectors to detect levels of reflected light in the NIR and red (670 nm) chlorophyll absorption band. This system used an artificial light source mounted with the system's sensor. Merritt et al. (1994) also used red and NIR reflectance to implement a weed spray system.

All of these sensor-applicators relied on differences in reflective properties of plants and soil in the red and near-infrared portion of the electromagnetic spectrum. Green chlorophyll producing plants absorb sunlight at red wavelengths, and reflect highly at near-infrared wavelengths. Soil tends to reflect more equally at both wavelengths.

Vegetation indices that take advantage of this difference in reflective properties work well in determining weeds from soil. The most commonly used index is the Normalized Difference Vegetative Index (NDVI) ((NIR-RED)/(NIR+RED)) introduced by Rouse et al. (1974) to separate green vegetation from its background soil brightness. Merritt et al. (1994) reported that NDVI based on percent reflectance worked well for consistent classification of plants from soil. Nitsch et al. (1991) compared four indices and found NDVI to be the best for differentiating living plant matter from soil. A variation of NDVI, the soil-adjusted vegetation index (SAVI) also uses red and near-infrared wavebands, but with added constants to minimize errors caused by soil brightness (Huete, 1988). Numerous other red and NIR VIs include the Transformed Vegetative Index (TVI) (Deering et al. 1975), the Ratio Vegetation Index (RVI) (Richardson and Wiegand, 1977), the Normalized Ratio Vegetation Index (NRVI) (Baret and Guyot, 1991), and the Perpendicular Vegetation Index (PVI) (Richardson and Wiegand, 1977).

While research using red and NIR sensing seems promising, attempts to implement this technology have yielded inconsistent results (Beck , 1996) due in part to variability in the landscape being sensed. Different soil types exhibit different reflective characteristics. Also, within a single soil type, soil color changes with soil conditions such as wet or dry, broken or crusted (Nitsch et al., 1991). In addition to changes in soil reflectance, spectral response from bindweed cover will change from plant to plant and over time as the plants mature. Changes in atmospheric conditions and solar radiation from one day to the next also add to the complexity of designing a usable detection system.

While reflectance of soil and green plants vary, they have characteristic and recognizable reflectance curves. However, an area that contains a plant surrounded by soil will produce a reflectance curve that does not appear like either, but rather a composite response, which is a combination of the two ground cover types. As the field-of-view is increased, the plant response is averaged out by the increasing soil response. If the field-of-view is too large, it becomes impossible to distinguish between an image containing plant and an image that does not. As a practical solution to this problem, a sensor's field-of-view must be small enough to reliably detect the smallest target weed on a soil background. At least one author has cited inability to detect small weeds as one of the problems facing selective spraying (Felton et al., 1991). On the other hand, small fields-of-view lead to increased system cost, because more sensors are necessary to cover the same amount of field area. Thus, the maximum field-of-view size that can reliably detect the target weed becomes a very important factor in the design of a viable weed detector.

Variations in spectral response due to differences in plants, soils, light level, and sensed areas containing both soil and green plant material have all caused problems for developers (Stone, 1994). A usable weed sensor must be able to readily distinguish viable weeds under all reasonable conditions. Its decision making process and field-of-view should be well defined in order to assure accuracy in detection. The objective of this research was to use a sensor simulation, based on spectrometer data from bindweed and soil to determine the maximum required sensor field-of-view by which NDVI can be reliably used to detect a target bindweed on bare soil.

Methods

Field-of-view size was calculated by a sensor simulation using bindweed and soil spectrometer data as input. The input data was collected on the Oklahoma State University Agricultural Experiment Station in Stillwater, Oklahoma on Sept. 11 and 23, and Oct. 2, 25, and 31, 1996. The field was a Bethany silt loam soil that had been tilled in mid-summer and the weeds allowed to grow back. The bulk of the vegetation present was field bindweed, along with smaller amounts of other weed species. Reflected solar energy between 500 and 1000 nm was measured over areas that were completely covered with bindweed and over bare soil. All experiments were conducted between 10:00 A.M. and 3:00 P.M. to minimize possible distortions associated with low solar zenith angles. In every case, the sensor was placed at a vertical position over the area being sensed, with no shadows in the field-of-view. Four sets of data, 9/11/96, 9/23/96, 10/2/96 Clear, and 10/25/96 Clear were collected in mostly sunny conditions. Data set 10/31/96 was taken on an overcast day directly before a storm, and data sets 10/2/96 Shadow and 10/25/96 Shadow were taken on sunny days with artificially created shadows. The artificial shadow was created with a plywood sheet covered in course finished black rubber. These artificial shadows were meant to simulate conditions when a sensor's target area was in a direct shadow, such as from an implement, trees, or nearby buildings.

Data were collected with an Ocean Optics model PC1000S spectrometer and a personal computer. A lawn tractor was used as the collection platform (fig. 1). Fiber optic cable connected the spectrometer mounted in the computer case to a sensor head at the front of the tractor. The sensor head was a sealed black box with a single hole drilled in the bottom. The edges of the hole created a sharp edge for the sensor's view of the ground. The spectrometer's field-of-view was controlled by the height of the sensor head from the ground. The sensor head was located 540 mm above the target. The area sensed was a 51 mm diameter circle with an area of 2030 mm^2.

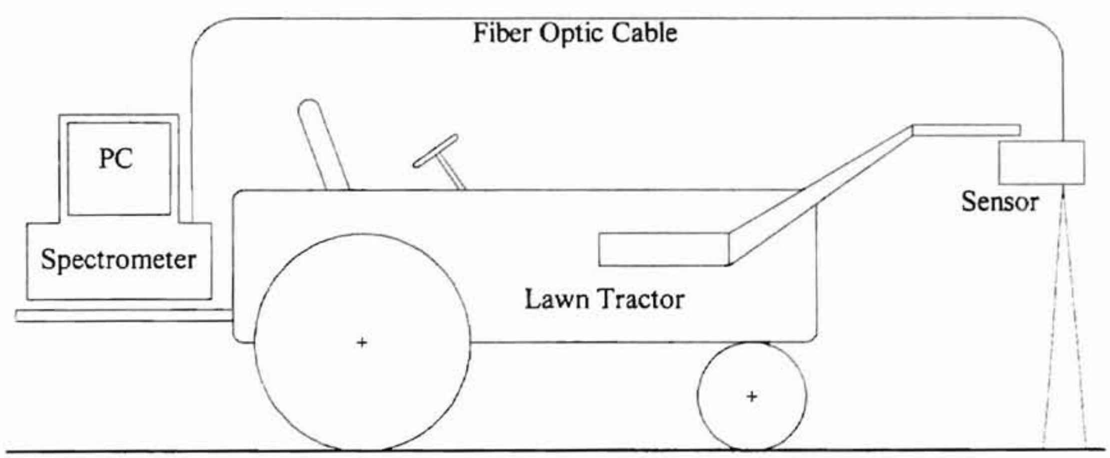

Figure 1—Lawn tractor field collection apparatus

Before a sensor field-of-view could be determined, it was necessary to define a target weed. The target weed was the smallest bindweed the sensor must consistently detect. It was defined as a single bindweed, having at least one runner approximately 150 mm long. This was the smallest bindweed recommended for chemical treatment (Landmaster BW label, 1997; Zollinger, 1996; Field bindweed official control program, 1988). The target weed was estimated to cover an area of 6090 mm^2; three times the size of a spectrometer image. If a weed of this size could be consistently detected, then larger weeds would also be detected, since they occupied more field-of-view area and were responsible for more of the sensor response.

Detection decisions were based on NDVI calculated from the spectrometer measurements. Red light in the wave band of 660 to 680 nm and near-infrared between 770 and 790 nm were extracted from the spectrometer data and averaged. Each of the seven field data sets was further divided into four sub-sets: red soil (RED_s), near-infrared soil (NIR_s), red bindweed (RED_b), and near-infrared bindweed (NIR_b). Chi squared goodness of fit tests indicated that the subset were not significantly different (0.05 level) from normal populations. Means, standard deviations, standard errors, and sums of the squares of deviation describing the samples of RED_s, RED_b, NIR_s, and NIR_b for each test condition were used as inputs for the sensor simulation.

Information about the correlation of red and NIR was also needed as simulation input. A linear regression model of NIR_s to RED_s and NIR_b to RED_b for each of the seven test conditions was also established.

Simulation

Assuming that the populations of bindweed and soil measurements were normal and were represented by the collected field samples, a simulation program was developed. For each of the seven data sets, the program simulated field measurements of reflected energy from bindweed and soil by multiple sensors, each with a different field-of-view. Sensor responses were simulated by summing RED and NIR measurements from a number of 51 mm diameter pixels, so that the total area of the summed pixels was equal to the desired area of the sensor field-of-view

To generate the values of each pixel (fig. 2), e.g. a soil pixel, a red value was randomly selected from the appropriate RED population. RED_s in the case of the soil pixel. Using the linear regression model, a corresponding prediction of NIR_s was found. Least squares method required that prediction error be normally distributed about the predicted NIR value. This error was calculated by Steel and Torrie (1980) as:

$$S_{\hat{y}} = S_{yx}^2\left[\frac{1}{n}+\frac{\left(x_O-\bar{x}\right)^2}{\sum\left(x-\bar{x}\right)^2}\right] \tag{1}$$

Where: s_{yx}^2 = error mean square
n = sample size
$\bar{x}$ = mean of x population
x_O = specific value of x.

All possible values of NIR_s for the randomly selected RED_s were described by a normal distribution with the regression predicted NIR_s as the mean and the error mean square as a measure of variance. Although RED and NIR correlated as a whole, no two bindweed or soils share exactly the same RED and NIR relationship. The specific relationship lay above or below the regression line somewhere inside the prediction error population. Therefore, for the simulation to be realistic, NIR_s values were selected randomly from the error population. RED_b and NIR_b were used if a bindweed pixel was required. This process was repeated to generate red and NIR values for each pixel in a field-of-view.

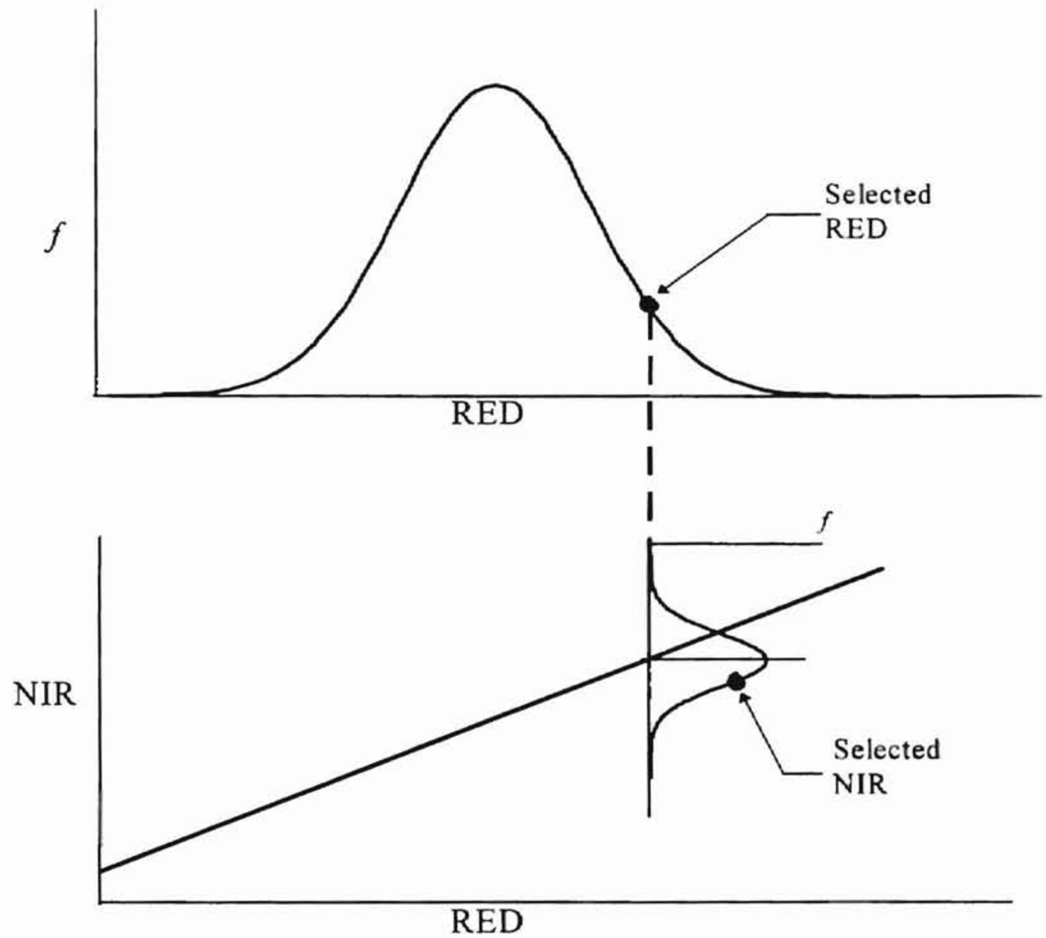

Figure 2—Simulation process to select RED and NIR values of a single pixel

The generated red and NIR pixel values were added to calculate composite values for an entire field-of-view. NDVI was calculated from these composites. NDVI for fields of-view containing the target bindweed on a soil background were calculated by:

$$NDVI = \frac{\sum_{1}^{BS} NIR_b + \sum_{1}^{DS} NIR_s - \sum_{1}^{BS} RED_b - \sum_{1}^{DS} RED_s}{\sum_{1}^{BS} NIR_b + \sum_{1}^{DS} NIR_s + \sum_{1}^{BS} RED_b + \sum_{1}^{DS} RED_s} \tag{2}$$

where: BS = number of bindweed pixels in field-of-view = user input
DS = number of soil pixels in field-of-view = FOV - BS
FOV = sensor field-of-view area expressed in number of pixels
NIR_b = near-infrared irradiance from bindweed population
RED_b = red irradiance from bindweed population
NIR_s = near-infrared irradiance from soil population
RED_s = red irradiance from soil population.

The target weed in all simulations was represented by three bindweed pixels ($BS = 3$). The remaining field-of-view was filled with soil pixels. In order to assess the level of detection for each field-of-view, it was necessary to also create equivalent sensor images with soil-only responses. Since $BS = 0$, and $DS = FOV$ in an all soil image, equation 2 was simplified to:

$$NDVI = \frac{\sum_{1}^{DS} NIR_s - \sum_{1}^{DS} RED_s}{\sum_{1}^{DS} NIR_s + \sum_{1}^{DS} RED_s} \tag{3}$$

The process described above was used to create 100 random measures of NDVI containing bindweed and 100 random measures of NDVI containing only soil for each simulated sensor field-of-view. The mean and standard deviation from each of these data sets of 100 were used to describe the two normal populations of possible sensor responses for a field-of-view: a bindweed inclusive NDVI population and a soil-only NDVI population (fig. 3). The decision of detection was made by whether a simulated sensor response was greater or less than a specific NDVI threshold. In theory, if a weed was present, NDVI was greater than the threshold. If there was no weed, NDVI was less than the threshold. Error was assessed when NDVI calculations fell incorrectly on the wrong side of the threshold. Two types of errors resulted: error in failing to detect bindweed when it was present, and falsely detecting soil when there was no bindweed present. For purposes of analysis, the former was held constant at levels of five and 10%, and the latter was calculated. NDVI threshold was calculated so that the appropriate percent (5 or 10%) of the bindweed inclusive population was less than threshold value. The error in falsely detecting soils was the percentage of the soil-only population that was greater than the threshold value. This error was calculated by (Steel and Torrie, 1980):

$$error = 1 - \left[\frac{1}{\sqrt{2\pi\sigma}} e^{-(y-\mu)^2/2\sigma^2} \right] \tag{4}$$

where: y = NDVI threshold
μ = mean of 100 soil-only simulated samples
σ = standard deviation of 100 soil-only simulation samples.

Errors from each field of view under each of the seven field conditions was assessed in this way.

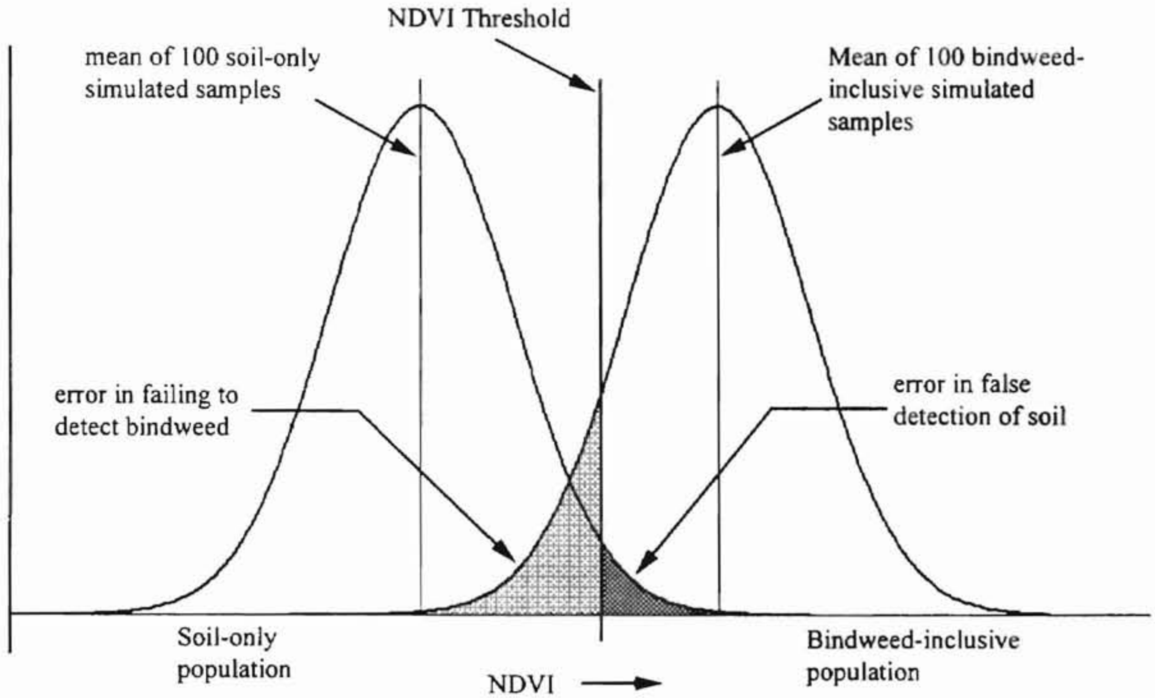

Figure 3—Threshold selection and error determination from simulation for a sensor field-of-view

The error versus field-of-view data from the simulation were compiled, and simple curves fit for error as a function of field-of-view for each of the seven ambient conditions. By knowing the size of the target weed, this analysis was converted to error as a function of the percentage of the field-of-view covered with bindweed.

To asses the contributions of variability in soil reflectance and solar intensity to changes in NDVI, incident solar illumination, rainfall, soil color, and clouds were measured or observed. Solar illumination during the sample times was collected from an Oklahoma Mesonet weather station on the same farm as the bindweed field. Rainfall events for the five days previous to each sample date were also measured at the Mesonet site. Observations of soil color and cloud cover were recorded during field collection.

Results and Discussion

Bindweed-only and soil-only spectrometer responses were easily distinguished for all conditions, both with NDVI and by visual inspection of reflectance curves over the entire band of the spectrometer. A typical reflectance curve for bindweed had a characteristic sigmoidal shape, showing high absorption in the 670 nm wavelength and reflectance in the 780 nm wavelength. A typical reflectance curve for soil was nearly a straight line, demonstrating more equal reflectance at both wavelengths (fig. 4). Error began to occur when images containing pixels of both ground cover types were examined.

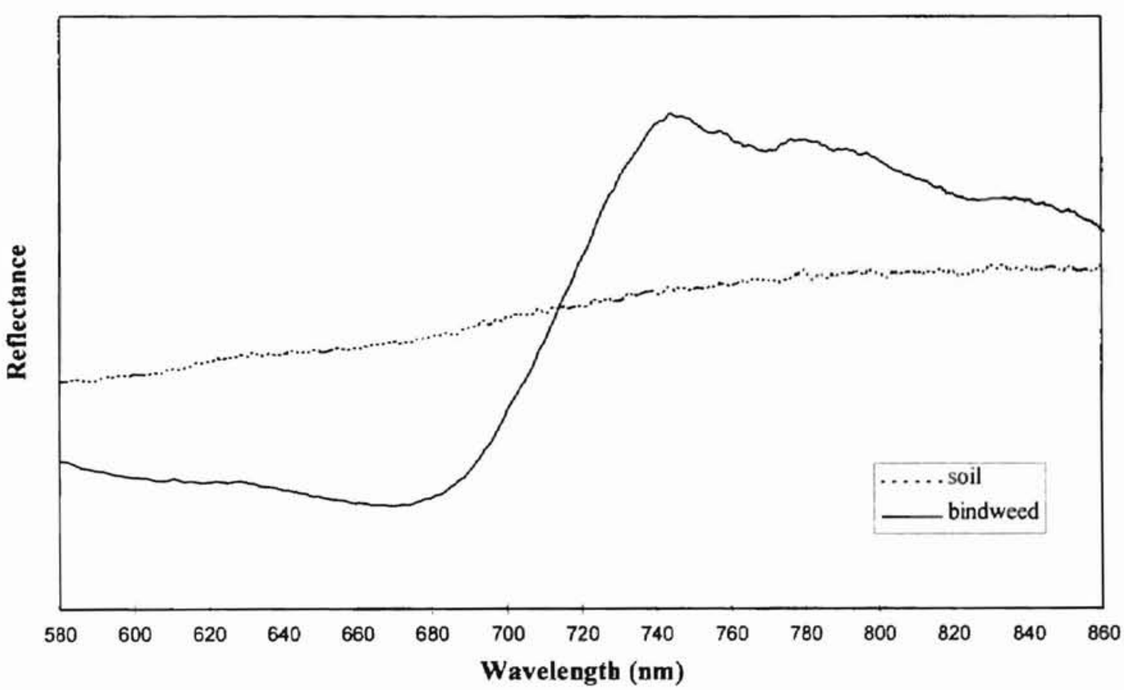

Figure 4—Typical reflectance curves for bindweed and soil from study field

Results of the simulations were expressed graphically by error as a function of the percentage of the sensor field-of-view covered by bindweed (fig. 5-11). Each point on these graphs simulated the result of a sensor field trial with a specific field-of-view, sampling 100 bindweed and 100 soil locations. A sample population NDVI threshold technique rather than an absolute NDVI threshold was used, so each point also has a unique threshold calculated for that set of simulated data. Each graph represents two levels of error in failing to correctly detect bindweed. The five percent error curve lay to the right of the 10% error curve as expected. The level of error in falsely detecting soil was read from the y-axis. If the x-axis were extended, both curves became asymptotic at zero error as the percent weed cover increased.

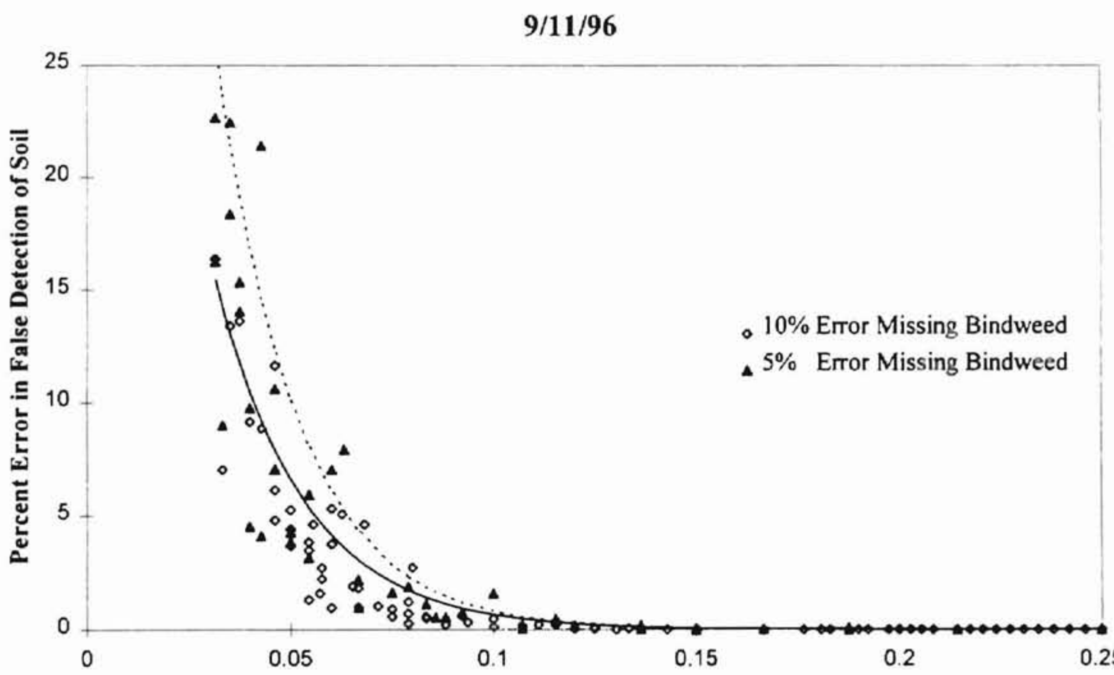

Figure 5—9/11/96—Error verses percent of field-of-view covered by bindweed

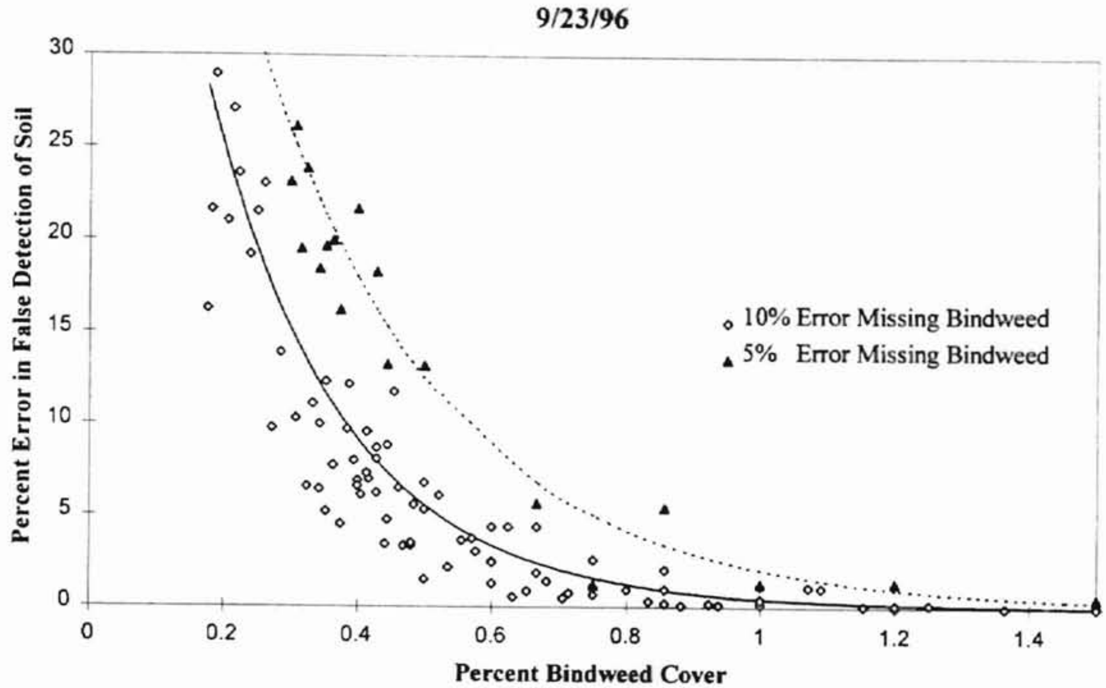

Figure 6—9/23/96—Error verses percent of field-of-view covered by bindweed

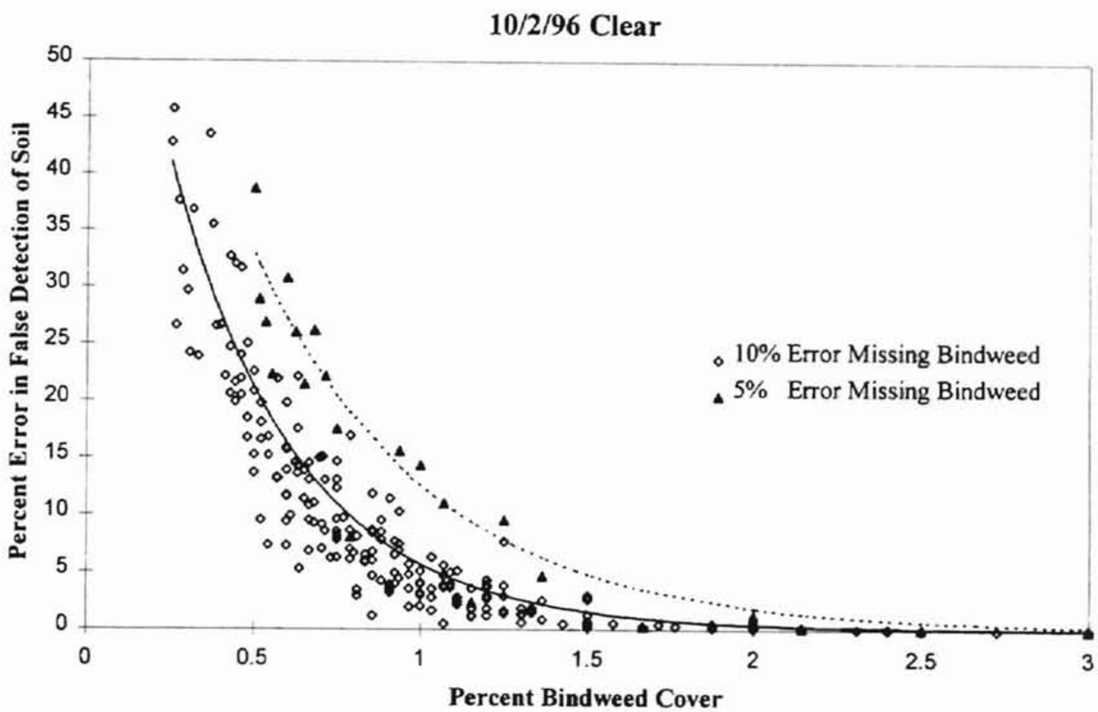

Figure 7—10/2/96 Clear—Error verses percent of field-of-view covered by bindweed

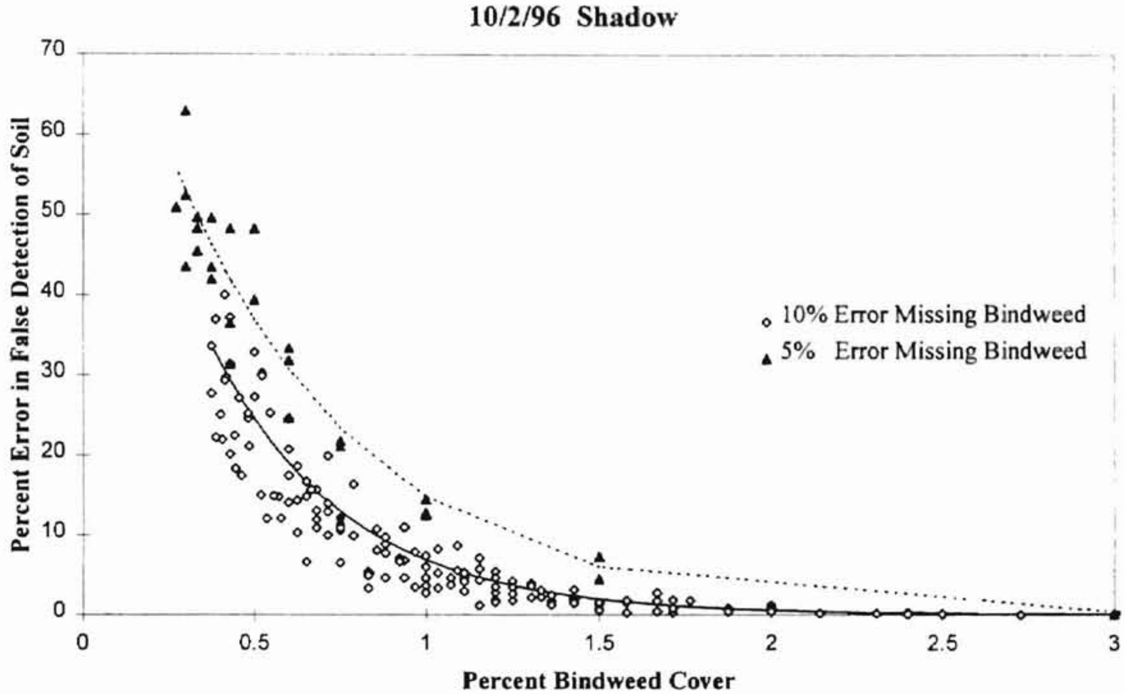

Figure 8—10/2/96 Shadow—Error verses percent of field-of-view covered by bindweed

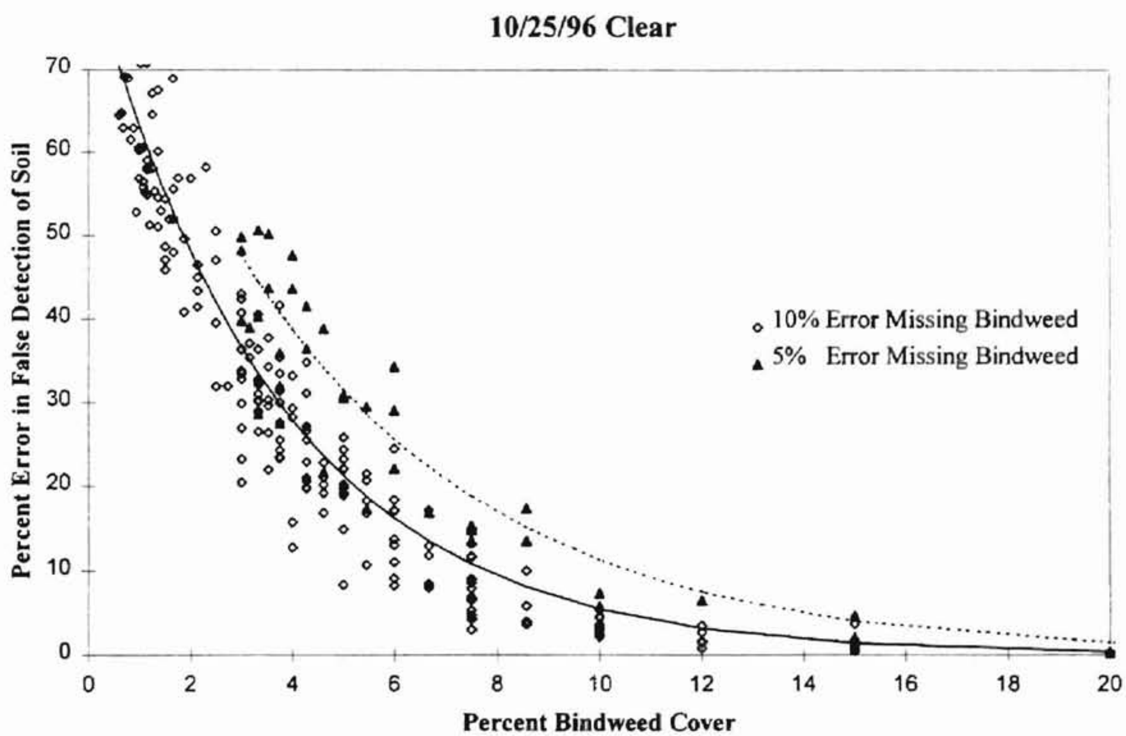

Figure 9—10/25/96 Clear—Error verses percent of field-of-view covered by bindweed

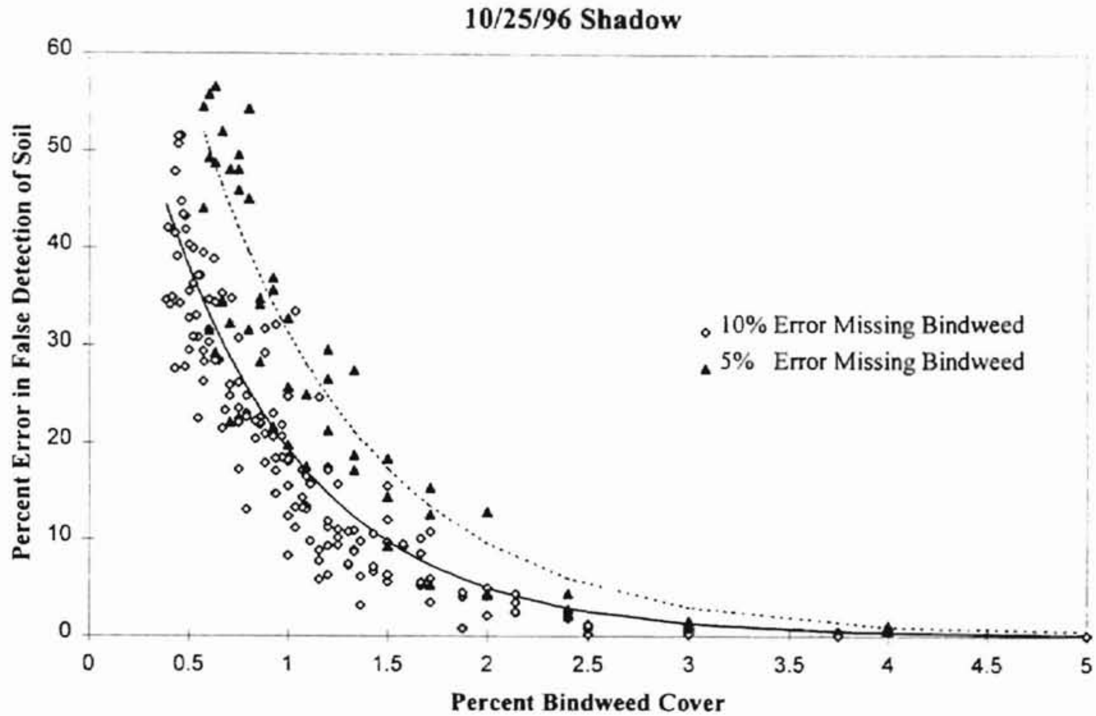

Figure 10—10/25/96 Shadow—Error verses percent of field-of-view covered by bindweed

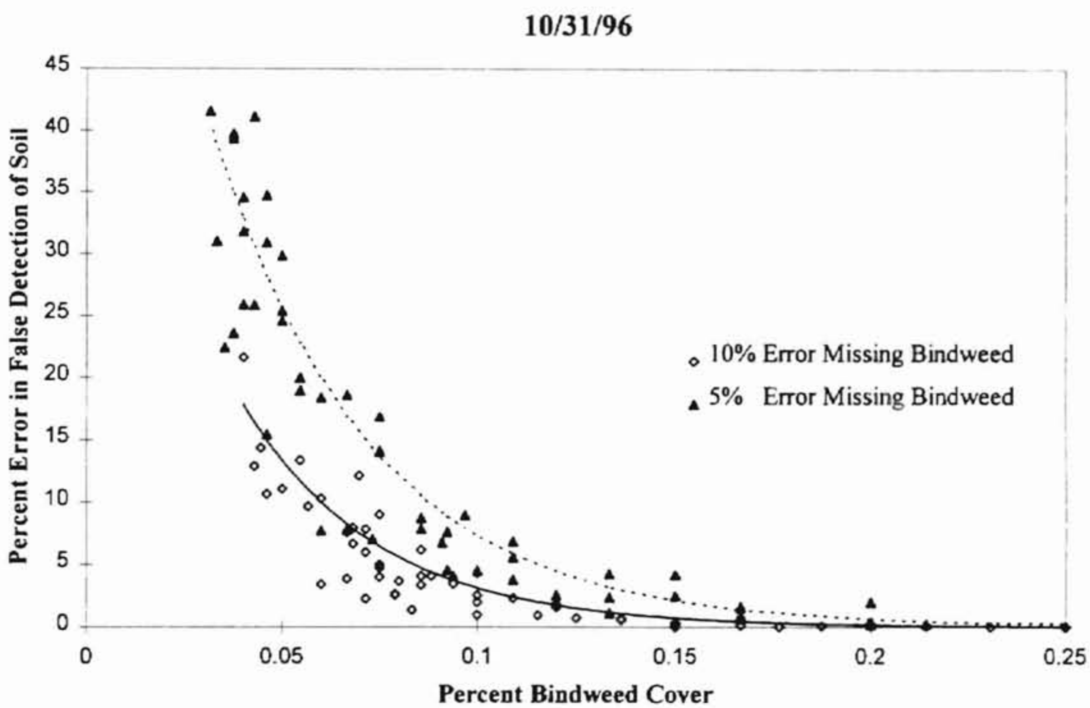

Figure 11—10/31/96—Error verses percent of field-of-view covered by bindweed

The error versus percent cover relationships were described by:

$$y = 100e^{(a+bx)} \tag{5}$$

where: y = percent error in falsely detecting bare soil
x = weed cover (percentage of field-of-view)
a and b = coefficients unique for each set of conditions (table 1).

Table 1. Error equation coefficients

Sample Set	5% error*		10% error*	
	a	*b*	*a*	*b*
9/11/96	0.2538	-50.8126	-0.4045	-46.2635
9/23/96	-0.2616	-3.6356	-0.3742	-5.0322
10/2/96 Clear	-0.1445	-1.9251	-0.2317	-2.6361
10/2/96 Shadow	-0.0898	-1.8163	-0.1372	-2.5370
10/25/96 Clear	-0.1251	-0.2060	-0.1868	-0.2721
10/25/96 Shadow	0.0175	-1.1800	-0.2887	-1.3536
10/31/96	-0.1133	-24.9945	-0.5607	-29.0590

* allowed error in failing to correctly detect bindweed

An economic study would be required to determine the optimum allowable amount of each type of error. This would ultimately determine the maximum field-of-view. Such a study was beyond the scope of this paper. For the remainder of this study, the optimum threshold was assumed to occur when both errors were equal and at a predetermined level.

Using the standard of equal errors, weed cover requirements varied greatly between the seven data sets (table 2). No single field-of-view was optimum for all conditions. The 10/25/96 Clear set was the worst case and required the smallest field-of-view. A field-of-view of 0.08 m^2 was required to detect the minimum target bindweed while maintaining errors of 10%. On average, nearly 8% of the field-of-view would have had to be bindweed before the sensor could correctly detect it. At the opposite extreme, a sensor on 9/11/96 would have required only 0.04% weed cover to maintain 10% error. The median required weed cover for all seven sets was 0.79% of the field-of-view with 10% error and 1.48% with 5% error. To detect a 6090 mm^2 bindweed, these correspond to fields-of-view of 0.77 m^2 and 0.41 m^2, respectively. The differences in percent cover requirements between days could be attributed to variability of the bindweed, soils, and light conditions both within and between data sets.

Table 2. Bindweed Simulation Results

Sample Set	5% error*		10% error*	
	Weed cover required (% of FOV)	Max. field of view† (m^2)	Weed cover required (% of FOV)	Max. field of view† (m^2)
9/11/96	0.06	9.51	0.04	14.82
9/23/96	0.75	0.81	0.38	1.59
10/2/96 Clear	1.48	0.41	0.79	0.77
10/2/96 Shadow	1.60	0.38	0.85	0.71
10/25/96 Clear	13.94	0.04	7.78	0.08
10/25/96 Shadow	2.55	0.24	1.49	0.41
10/31/96	0.12	5.27	0.06	10.14

* Assumes equal error in failing to correctly detect bindweed and falsely detecting soil

† Based on target bindweed of simulation (6090 mm^2)

Although NDVI did correct for some sunlight variability, it did not correct entirely (Lillesand and Kiefer, 1994). At least some of the variability in field-of-view determination could be attributed to changes in sunlight conditions during sampling.

Oklahoma Mesonet irradiance data, averaged over 15 minute intervals, indicated that there was some variability in total brightness levels between days, and considerable variability in sunlight conditions during the Sept. 23, and Oct. 31, data collection. However, there was no correlation between this data and calculated field-of-view size. Variable and fast moving cloud cover was observed during collection of the 10/25/96 data and could have contributed to the large field-of-view calculated for that day.

Variability in weed samples measured also played a part in the field-of-view differences between sets. While bindweed has a distinctive spectral pattern, it is not absolute for every plant of the species (Lillesand and Kiefer, 1994). No two bindweed plants reflect exactly the same, due to factors such as health, leaf structure, morphology, moisture, and the level of photosynthesis.

Physical differences in the color, surface roughness, and moisture content of the soil also existed and contributed to the variability in field-of-view. There was considerable surface roughness from tillage. Since the areas being sensed were small, clods, rills, and washouts could have contributed to variability of the data.

Variability of color between the soil samples was also observed. Color and moisture content were very much interrelated. Soil moisture content can cause large changes in soil color and therefore, reflectance in the visible portion of the spectrum. Also water in soil absorbs energy in the near-infrared wavelengths (Lillesand and Kiefer, 1994). Wetting or drying of the background soil, could dramatically change the amount of NIR and RED reflectance thereby changing NDVI values. After a rainfall event, it is natural to see areas of the field where drying is occurring faster that others. Under these conditions, since there is more than usual variability in soil surface moisture, it is expected that NDVI should be more variable. Rainfall events of varying degrees occurred within the five days prior to each collection date with the exception of 9/11/96, but there was no correlation between the amount of rainfall and field-of-view size. A rainfall of 36.6 mm occurred three days previous to the Oct. 25 data collection. This was more than twice the amount received in the five days previous to any other sample date.

In addition to the variability of physical differences among targets areas and environments, some error from instrumentation and experimental procedure may have also occurred. A small amount of error was apparent in the spectrometer images, indicated by the rough appearance of the response curves (fig. 4). This error is insignificant when compared to the amplitude of the over all response. The sample data, used as inputs for the simulation, were collected under actual field conditions and were chosen as representative of the field. Neither the soil or the bindweed was prepared or altered for the study, and all data was collected during a time of year when bindweed would normally be detected and sprayed in Oklahoma.

Conclusions

It was possible to distinguish between images containing a single target bindweed on a soil background from images of bare soil without bindweed. However, as image size increased beyond the size of the target plant, distinguishing the two became more difficult. With increasing image size, bindweed response was averaged out by the increasing soil response.

The median required bindweed cover for all test conditions was 0.79% of the field-of-view to maintain 10% average error in both failing to detect bindweed and falsely detecting soil. To maintain no greater than five percent error, bindweed must fill 1.48% of the field-of-view. The maximum required bindweed cover for any test condition with 10% error was 7.78%, and the minimum was 0.04%. A field-of-view of 0.08 m^2 will reliably detect the target bindweed (6090 mm^2) under all conditions tested with average errors no greater than 10%.

Variability in sensor measurements was due to differences in bindweed plants, soil locations, and the sunlight striking these targets. The influence of each of these factors was not quantified. No cause and effect relationship could be established between rainfall events or sunlight variability and percent cover requirements. It was likely that variation in soil reflectance was a greater factor than variation in bindweed, because soil accounted for a larger percentage of the field-of-view and had more influence on the NDVI.

No single field-of-view area was optimum for all sets of test conditions. A means of accounting for soil and sunlight variability should produce more uniform results.

References

Baret, F. and G. Guyot. 1991. Potentials and limits of vegetation indices for LAI and APAR assessment. *Remote Sensing the Environment* 35:161-173.

Beck, J. 1996. Reduced herbicide usage in perennial crops, row crops, fallow land and non-agricultural applications using optoelectronic detection. SAE Paper No. 96-

1758. Warremdale, PA.: SAE.

Deering, D. W., J. W. Rouse, R. H. Haas, and J. A. Schell. 1975. Measuring :forage production" of grazing units from Landsat MSS data. In *Proceedings of the 10th International Symposium on Remote Sensing of Environment, II,* 1169-1178.

Felton, W. L., A. F. Doss, P. G. Nash and K. R. McCloy. 1991. A microprocessor controlled technology to selectively spot spray weeds. In *Proc. Automated Agricultural for the 21st Century Symposium*, 427-432. Chicago, IL.

"Field bindweed, *Convolvulus arvensis*". *Utah State University Extension noxious weeds list*. <//ext.usu.edu/ag/weeds/fbind.htm> (Jan. 1998).

Field bindweed official control program. 1988. K.A.R. 4-8-29. Topeka, KS: Kansas Department of Agriculture.

Huete, A.R. 1988. A soil-adjusted vegetation index(SAVI). *Remote Sensing of Environment* 25:295-309.

LandMaster BW label, Monsanto 1997 Crop Chemical and MSDS Book, 1997. Pages 163-67.

Lillesand, T. M. and R. W. Kiefer. 1994. *Remote Sensing and Image Interpretation.* New York: John Wiley & Sons, Inc.

Majek, B. A. 1993 Bindweed identification and control. FS676. New Brunswick, NJ.: Rutgers Cooperative Extension.

Merritt, S. J., G. E. Meyer, K. Von Bargen, and D. A. Mortensen. 1994. Reflectance sensor and control system for spot spraying. ASAE paper no. 94-1057. St. Joseph, MI.: ASAE.

Nitsch, B. B., K. Von Bargen, G. E. Meyer, and D. A. Mortensen. 1991. Visible and near-infrared plant, soil and crop residue reflectivity for weed sensor design. ASAE Paper No. 91-3006. St. Joseph, MI.: ASAE.

Richardson, A. J., C. L. Wiegand. 197. Distinguishing vegetation from soil background information. *Photogramnetric Engineering and Remote Sensing* 43(12):1541-1552.

Rouse, J. W. Jr., R. H. Haas, D. W. Deering, J. A. Schell, and J. C. Harlan. 1974. Monitoring the venal advancement and retrogradation (green wave effect) of natural vegetation. In *NASA/GSFC Type III Final Report*, 371. Greenbelt, MD.

Steel, R. G. D. and J. H. Torrie. 1980. *Principles and Procedures of Statistics: A Boimetrical Approach*. New York: McGraw-Hill, Inc.

Stone, M. L. 1994. Embedded neural networks in real time controls. SAE Paper No. 94 1067. Warrendale, PA.: SAE.

Zollinger, R. K. and R. G. Lym. 1996. Identification and control of field bindweed. W802. Fargo, ND: North Dakota State University Extension Service.

Chapter III

Field-of-view Determination for a Bindweed Detection Sensor

Abstract

One alternative to the present method of uniform herbicide application is to selectively spray only the weeds in a field. Control of field bindweed, *Convolvulus arvensis,* in fallow winter wheat is a prime application for such technology. This research was conducted, using a photoelectric diode sensor, to determine the maximum required sensor field-of-view by which the Normalized Difference Vegetative Index (NDVI) can be reliably used to detect a target size bindweed on bare soil.

Eleven fields-of-view between 0.065 and 0.710 m^2 were compared to determine what image size containing a single target bindweed on bare soil could be distinguished from images that contained only soil. Irradiance was measured in the 670 nm and 780 nm nominal wavelengths. A reflectance based NDVI was calculated and used to distinguish soil and plant.

Image size and the sensor's ability to adjust for background variability were related. When soil and bindweed images were paired, it was possible to distinguish between images containing a single six inch bindweed from images of its surrounding soil for all fields-of-view. Detection was 100% for nine of the 11 fields-of-view and 98% for the other two. When soil and bindweed images were unpaired, a single NDVI threshold was used to distinguish between the two with some error. Error in not detecting bindweed increased as the decision threshold increased. Error in falsely spraying soil decreased as the decision threshold increased. The optimum threshold was defined as the intersection of the two error curves. Threshold error increased from 16.0 to 45.0% with increasing image size.

Soil moisture was a significant factor in NDVI variability. Threshold error was decreased slightly over the unpaired analysis when samples were classified by visually distinguishing between wet and dry soils.

Keywords: weed, detection, sensor, irradiance, reflective light

Introduction

Every year farmers throughout the world spend millions of dollars on tillage and herbicide in an attempt to control undesirable weed species in crop fields. In much of the United States, one of the most serious and difficult weed problems is field bindweed, *Convolvulus arvensis* (Field bindweed, *Convolvulus arvensis,* 1998). Bindweed is a member of the Morning-glory family and has multiple lateral runners, a long taproot, and arrow shaped leaves. Dense infestations of field bindweed may reduce crop yields by 50 to 60% (Zollinger, 1996). Tillage is the most widely accepted method of control, but to effectively control bindweed requires months of regular tillage operations (Majek, 1993). Occasional tillage may in fact help spread the weed and make problems worse.

The alternative to tillage weed control is chemical herbicides. Currently chemical herbicides are applied uniformly across an entire field which may have only a sparse or patchy population of weeds. To insure weed control, large amounts of chemical are applied, much of which falls on weed-free areas and will never reach the target plant. A large percentage of the herbicide, and consequently the farmer's money, is wasted. This waste of herbicide has a very real and negative effect on the profitability of crop production, as well as a potentially adverse environmental impact.

In an era of increasing operating costs, heightened awareness of environmental impact, and escalating regulation of agri-chemicals, a more efficient and environmentally conscious method of herbicide application is needed. One alternative to the usual method of uniform application is to selectively spray only the weeds in a field. With improving technology, it may now be possible to detect and spray weeds on the go using remote sensors and intermittent chemical applicators. A site specific herbicide system would utilize remote sensed data from either on-board sensors or overhead imagery to develop a vegetative index (VI) for small areas, or elements, of a field. Based on the index, the system would then make a decision of the presence or absence of a weed in each field element. This decision would be translated to a spray command and carried out by computer controlled applicators.

Bindweed control in winter wheat is a prime application for such technology. Bindweed can be treated in late summer or early fall, when winter wheat fields are fallow, and it can be reliably assumed that any growing plants are weeds. The task of the sensor and controller is then simply sense and determine what is plant and should be sprayed from what is soil and should not.

A number of systems sensing electromagnetic energy have been developed in an attempt to detect and selectively spray weeds. Stone (1994) used an optical sensor and an artificial neural network to detect bindweed. This sensor measured reflected energy in three bands: green, red, and near-infrared (NIR). This unit was able to detect 92% of the cases where weeds were present and reject 80% of the cases where weeds were not present. Felton et al. (1991) developed a spray system with remote sensors that also used reflected energy in the red and near-infrared wavebands as a means of distinguishing between plants and soil. He estimated the mean reduction in area sprayed was 90%. Beck (1996) reported on a second selective sprayer that used silicon PIN photodetectors to detect levels of reflected light in the NIR and red (670 nm) chlorophyll absorption band. This system used an artificial light source mounted with the system's sensor. Merritt et al. (1994) also used red and NIR reflectance to implement a weed spray system.

All of these sensor-applicators relied on differences in reflective properties of plants and soil in the red and near-infrared portion of the electromagnetic spectrum. Green chlorophyll producing plants absorb sunlight at red wavelengths, and reflect highly at near-infrared wavelengths. Soil tends to reflect more equally at both wavelengths.

Vegetation indices that take advantage of this difference in reflective properties work well in determining weeds from soil. The most commonly used index is the Normalized Difference Vegetative Index (NDVI) ((NIR-RED)/(NIR+RED)) introduced by Rouse et al. (1974) to separate green vegetation from its background soil brightness. Merritt et al. (1994) reported NDVI based on percent reflectance worked well for consistent classification of plants from soil. Nitsch et al. (1991) compared four indices and found NDVI to be the best for differentiating living plant matter from soil. A variation of NDVI, the soil-adjusted vegetation index (SAVI) also uses red and near-infrared wavebands, but with added constants to minimize errors caused by soil brightness (Huete, 1988). Numerous other red and NIR VIs include the Transformed Vegetative Index (TVI) (Deering et al. 1975), the Ratio Vegetation Index (RVI) (Richardson and Wiegand, 1977), the Normalized Ratio Vegetation Index (NRVI) (Baret and Guyot, 1991), and the Perpendicular Vegetation Index (PVI) (Richardson and Wiegand, 1977).

While research using red and NIR sensing seems promising, attempts to implement this technology have yielded inconsistent results (Beck , 1996) due in part to variability in the landscape being sensed. Different soil types exhibit different reflective characteristics. Also, within a single soil type, soil color changes with soil conditions such as wet or dry, broken or crusted (Nitsch et al., 1991). In addition to changes in soil reflectance, spectral response from bindweed cover will also change from plant to plant and over time as the plants mature. Changes in atmospheric conditions and solar radiation from one day to the next also add to the complexity of designing a usable detection system.

While reflectance of soil and green plants vary, they have characteristic and recognizable reflectance curves. However, an area that contains a plant surrounded by soil will produce a reflectance curve that does not appear like either, but rather a composite response, which is a combination of the two ground cover types. As the field-of-view is increased, the plant response is averaged out by the increasing soil response. If the field-of-view is too large, it becomes impossible to distinguish between an image containing plant and an image that does not. As a practical solution to this problem, a sensor's field-of-view must be small enough to reliably detect the smallest target weed on a soil background. At least one author has cited inability to detect small weeds as one of the problems facing selective spraying (Felton et al., 1991). On the other hand, small fields-of-view lead to increased system cost, because more sensors are necessary to cover the same amount of field area. Thus, the maximum field-of-view size that can reliably detect the target weed becomes a very important factor in the design of a viable weed detector.

Variations in spectral response due to differences in plants, soils, light level, and sensed areas containing both soil and green plant material have all caused problems for developers (Stone, 1994). A usable weed sensor must be able to readily distinguish viable weeds under all reasonable conditions. Its decision making process and field-of-view should be well defined in order to assure accuracy in detection. The objective of this research was to determine the maximum required sensor field-of-view by which NDVI can be reliably used to detect a target size bindweed on bare soil.

Methods

Sensor data from 11 sizes of field-of-view were compared to determine the maximum field-of-view where an image containing a single target bindweed on a soil background could be distinguished from images that contained only soil. The data were separated into pairs of one bindweed image and one soil image for each field-of-view. Both images came from the same area in the field at approximately the same time.

The target weed, the smallest bindweed the sensor must consistently detect, was defined as a single bindweed having at least one runner approximately six inches long. This is the smallest bindweed recommended for chemical treatment (Landmaster BW label, 1997) (Zollinger, 1996) (Field bindweed official control program, 1988). Target weeds sampled during this study, when viewed from above, ranged in area from 1300 mm^2 and 10700 mm^2, with a mean of 3900 mm^2. If a weed of this size could be consistently detected, then larger weeds would also be detected, since they occupied more field-of-view area and were responsible for more of the sensor response.

The normalized difference vegetative index (NDVI) was selected as the vegetative index for this application. The use of NDVI was advantageous because it helped compensate for changes in target illumination (Lillesand and Kiefer, 1994). The nominal wavelengths of 670 nm (red) and 780 nm (NIR) were used to calculate NDVI. These frequencies were consistent with past research and corresponded with the wavelengths used in a nitrogen detection sensor also in development at Oklahoma State University (Stone et al., 1996). Visual inspection of bindweed and soil reflectance curves taken with a spectrometer verified the appropriateness of these wavelengths and the use of NDVI (Criner, 1998). However, NDVI did not completely eliminate the effects of variable illumination (Lillesand and Kiefer, 1994). To compensate for this variability, NDVI was calculated based on percent reflectance. Irradiance of the field element and a spectrally white reference plate were taken simultaneously. Reflectance NDVI was calculated as:

$$NDVI_{reflectance} = \frac{\left(\frac{NIR_{target}}{NIR_{ref}} - \frac{RED_{target}}{RED_{ref}}\right)}{\left(\frac{NIR_{target}}{NIR_{ref}} + \frac{RED_{target}}{RED_{ref}}\right)} \qquad (1)$$

Previous simulation work with spectrometer data (Criner, 1998) suggested a sensor should reliably detect a target bindweed in a 0.08 m^2 field-of-view under most field conditions. A slightly smaller square image size of 0.065 m^2 was chosen as the minimum field-of-view. A 0.710 m^2 image, 11 times the minimum, was selected as the maximum size.

A photoelectric diode sensor developed at Oklahoma State University was used to measure reflected energy from the sample areas in the 664 to 676 nm and 774 to 786 nm wavebands (fig. 1). The sensor measured two red and two NIR channels. One pair of red and NIR channels measured reflected energy from the soil/plant target. The second pair measured energy reflected from a spectrally white reference plate mounted above the sensor.

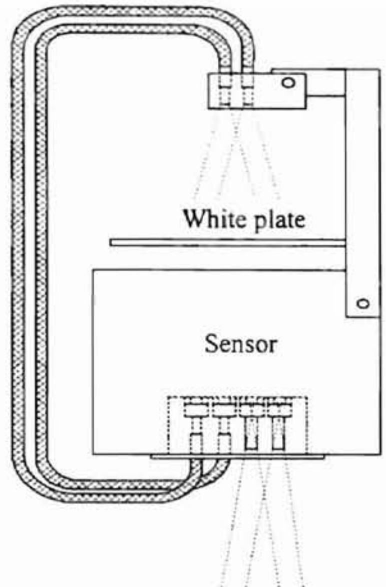

Figure 1--Photoelectric diode sensor

A sensor height of 0.99 m from the bottom of the sensor to the ground was chosen for these experiments. This provided a square field-of-view on the ground of 0.25 m by 0.25 m. The field-of-view was determined by reflecting a narrow strip of light from a light bar onto a white paper positioned under the sensor. Sensor response was recorded as the light strip was slowly passed from side to side and front to back under the sensor. The image size was defined as the area which contained 95% of the sensor response (fig. 2).

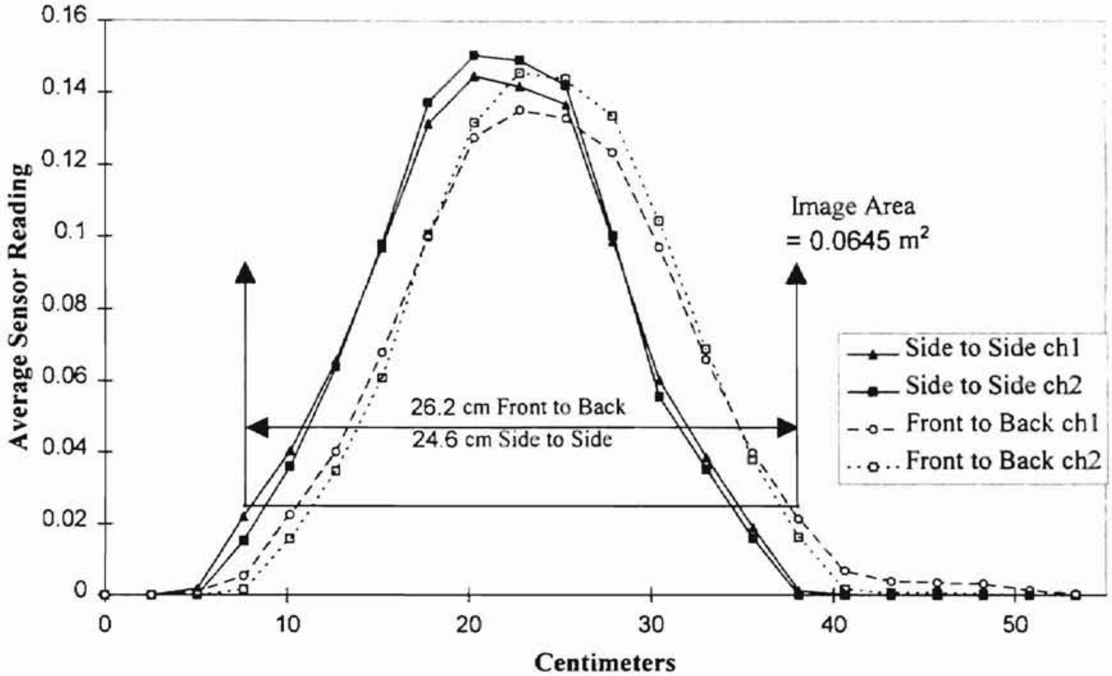

Figure 2--Sensor Response Curves for Sensor Image Size Determination

The sensor was mounted on a 3.7 m long angle iron frame (fig. 3). The sensor could be traversed the length of the frame to collect 11 contiguous 0.065 m^2 images with a single positioning of the frame .

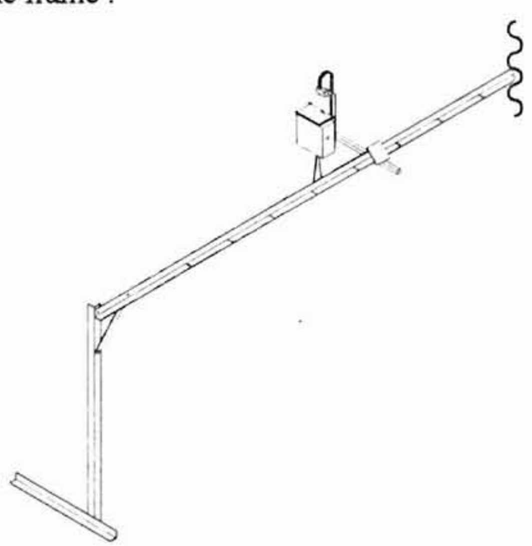

Figure 3--Sensor mounted on angle frame

During the fall on 1997, 49 data sets were collected to define field-of-view size of the bindweed detection sensor. Sensor fields-of-view of 0.065, 0.129, 0.194, 0.258, 0.323, 0.387, 0.452, 0.516, 0.581, 0.645, and 0.710 m^2 were examined. The data was collected in a field infested with bindweed on the Oklahoma State University Agricultural Experiment Station in Stillwater, Oklahoma on Oct. 2, 3, 6, 15, 17, and 22, 1997. Data were collected during the hours of 10:00 A.M. and 3:30 P.M. to minimize lighting problems that might originate from extremely low solar angles. The field was a Bethany silt loam soil that was fallow through the summer. It had been last tilled in mid-summer and the weeds allowed to grow back. The bulk of the vegetation present was field bindweed along with smaller amounts of other weed species.

Each sample set was a 0.25 m by 2.79 m transect (fig. 4) consisting of 11 individual 0.065 m^2 sensor images. The center image contained the target bindweed, and 5 images containing only bare soil were located on either side.

West ======> East

SOIL 10	SOIL 9	SOIL 8	SOIL 7	SOIL 6	BIND WEED	SOIL 5	SOIL 4	SOIL 3	SOIL 2	SOIL 1

Figure 4--Layout of field transect

Transects were oriented East to West with the sensor facing south. This orientation eliminated any interference that might occur due to shadows from the sensor or frame during testing. Sensor measurements were begun at the east end of the transect (SOIL 1), and the sensor was incremented 0.25 m west with each additional measurement. Twenty irradiance measurements were collected and averaged for each square. Locations of the transects in the field were arbitrary and were selected only by the presence of a target bindweed. In all cases, the area along the transect was cleared of all extraneous vegetation other than the target. The target and surrounding soil surface were disturbed as little as possible to maintain the sample in a natural state.

After the field data were collected, the raw data for each square in a transect was averaged and converted to a common unit by multiplying by the individual channel gains. A visual basic program was written to collect the data by field-of-view size and calculate reflectance NDVI.

NDVIs for fields-of-view of 0.065, 0.129, 0.194, 0.258, 0.323, 0.387, 0.452, 0.516, 0.581, 0.645, and 0.710 m^2 were calculated for each transect. Fields-of-view of 0.065 m^2 were taken directly from the transects as the image containing the target bindweed (BINDWEED in fig. 4). Fields-of-view larger than 0.065 m^2 were created by adding the red and NIR measurements of the target image and one or more contiguous soil images (fig. 5) to calculate a single NDVI for the entire area.

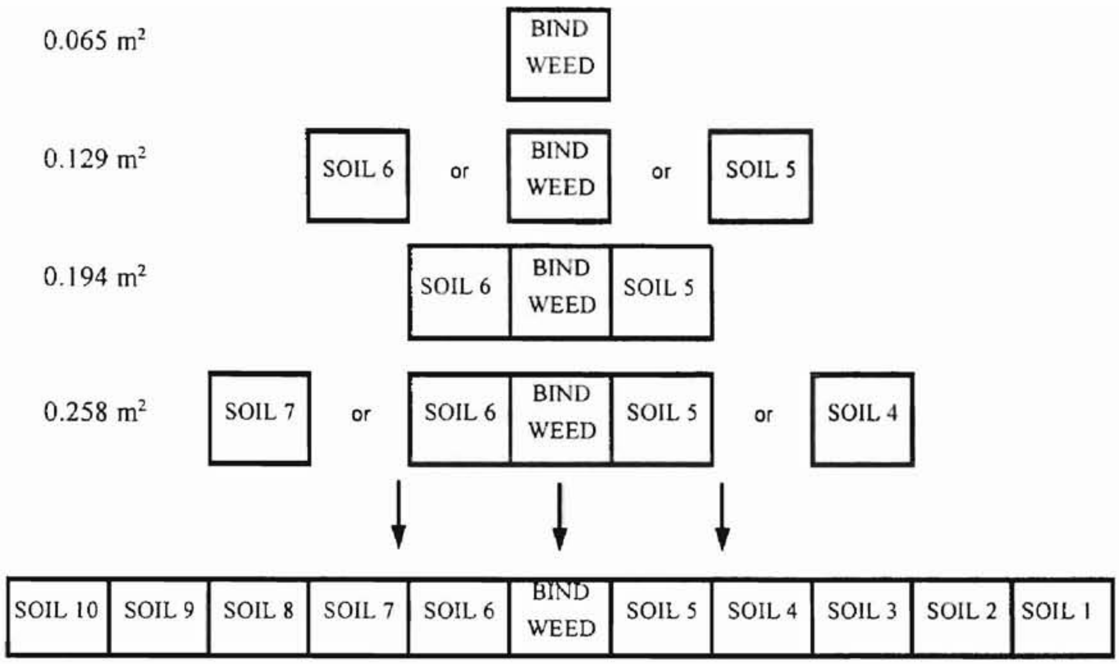

Figure 5--Creation of fields-of-view by adding contiguous 0.065 m^2 sensor readings

Equivalent size fields-of-view containing only soil were also created from each transect in order to compare bindweed and soil-only images. These images were created by randomly sampling each transect for the appropriate number of soil-only images and then adding together the sensor readings as described above. The result was 49 pairs of sensor images for each of the 11 fields-of-view. Each pair consisted of a bindweed plus background soil image and a background soil-only image.

A paired t-test was conducted for each image size to determine if images containing bindweed could be distinguished from associated soil-only images. This test, by design, eliminated the variability between transects by calculating the variance of the differences of the pairs rather than of the individual images. The t-test was conducted following the procedure given in Steel and Torrie (1980) with the null hypothesis of the difference between the pairs was zero.

An unpaired comparison of the data was also done to determine at what image size a single NDVI plant-soil threshold could be reliably used for detection. Theoretically, if a plant was within the sensor's view, the NDVI value would be above the threshold. If an image's NDVI was below the threshold value, no plant is present. Errors result when a NDVI reading falls incorrectly on the wrong side of the threshold. Any error was a result of variability in the soils and plants being sensed, since changes in light intensity were already accounted for in the calculation of NDVI. There were two types of expected error: error in falsely detecting bare soil and error in failing to correctly detect bindweed.

Errors for each field-of-view were calculated over a NDVI threshold range of 0 to 0.5. It was assumed that the 49 sets of sensor data were representative of the population of images possible for the field. For each image size, error in failing to detect bindweed or falsely detecting soil was determined based only on the sample information. Both types of error were calculated by:

$$Error = 100 * \left(\frac{i}{n} \right) \tag{2}$$

Where $Error$ = error in failing to detect bindweed
i = number of images containing bindweed with NDVI < threshold
n = number of samples

Where $Error$ = error if falsely detecting soil
i = number of images with out bindweed with NDVI > threshold
n = number of samples

An approach where threshold was adjusted based on gross changes in background response was also considered. Since it has been shown that soil reflectance values change due to surface moisture (Nitsch et al., 1991), the soil data were classified as moist or dry based on visual appearance. Twenty-nine transects were classified as dry, and 20 were classified as moist. An ANOVA test (GLM, SAS) verified that there was a significant difference between the two classes. A second unpaired analysis was conducted on each class to establish if adjusting the threshold NDVI value by class would reduce error.

Results and Discussion

Typical response curves generated in this study (fig. 6) demonstrated changes in NDVI as field-of-view changed. At the smallest field-of-view, the NDVI of images containing bindweed and those without were easily distinguished, because the bindweed occupied a significant portion of the image. As the field-of-view increased, the difference between the responses diminished. The soil-only NDVI remained essentially constant as the bindweed image NDVI decreased. It was possible to distinguish between responses at large image sizes, but to implement these sizes on a functioning sensor/applicator system will require a sensor with a high degree of precision. Also, since the differences between bindweed and soil images were small, any change in conditions that was not readily accounted for, e.g. a machine shadow crossing the sensor area may cause an error in detection. The range of NDVI readings for the two transects in figure 6 were entirely different. The bindweed image responses in figure 6a were for the most part lower than the soil responses in figure 6b. This demonstrated that while it was possible to distinguish between bindweed and soil responses under the same conditions, it was necessary to adjust the decision criteria in accordance with changes in conditions.

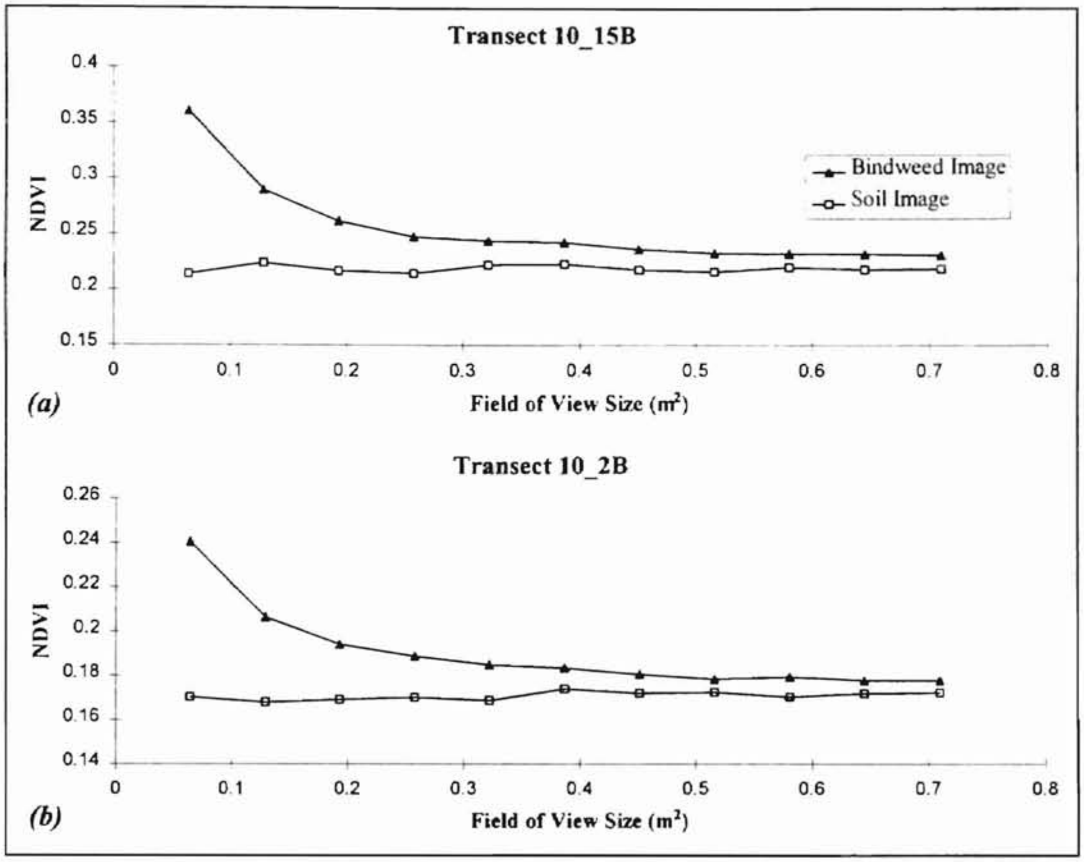

Figure 6--Typical sensor response; with and without bindweed for 11 fields-of-view. Transects from 10/2/97 and 10/15/97

Results from the paired t-test demonstrated the detection ability of the sensor was adequate for all fields-of-view tested. The null hypothesis of the mean of the sample differences was zero, was rejected for all 11 fields-of-view (table 1). For every image size tested, it was possible to distinguish between images containing a single six-inch bindweed on a soil background from images of the same soil without the bindweed. The sensor could differentiate between soil and bindweed images for all 49 samples in nine out of the 11 fields-of-view. The sensor failed to correctly distinguish between bindweed and soil once at 0.129 m^2 and once at 0.194 m^2. Thus, detection error was zero for nine fields-of-view, and two percent for the remaining two.

Table 1. Results of paired t-test and sample set detection error

Image Area (m^2)	Weed Cover* (% field-of-view)	Student's t	Probability (T<=t) two-tail	H_o**	Detection Error (%)
0.065	6.0	12.287	1.97E-16	reject	0
0.129	3.0	11.613	1.52E-15	reject	0
0.194	2.0	11.121	6.98E-15	reject	2
0.258	1.5	10.821	1.79E-14	reject	2
0.323	1.2	11.235	4.89E-15	reject	0
0.387	1.0	11.238	4.84E-15	reject	0
0.452	0.9	11.990	4.82E-16	reject	0
0.516	0.8	10.246	1.14E-13	reject	0
0.581	0.7	11.842	7.53E-16	reject	0
0.645	0.6	11.129	6.81E-15	reject	0
0.710	0.5	11.514	2.06E-15	reject	0

* Calculated from average bindweed size of 3900 mm^2
** H_o: Mean of sample differences is 0 for a given image size
$\alpha = 0.01$

Results of the unpaired analysis of the entire data set yielded two intersecting error curves (fig. 7). Error in not detecting bindweed increased as the decision threshold increased. Error in falsely detecting soil decreased as the decision threshold increased. Both types of error were approximated by sigmoidal curves described by:

$$y = \frac{A + B}{1 + e^{-(x-C)/D}} \tag{3}$$

where: y = error
x = NDVI
A, B, C, and D are unique coefficients (table 2).

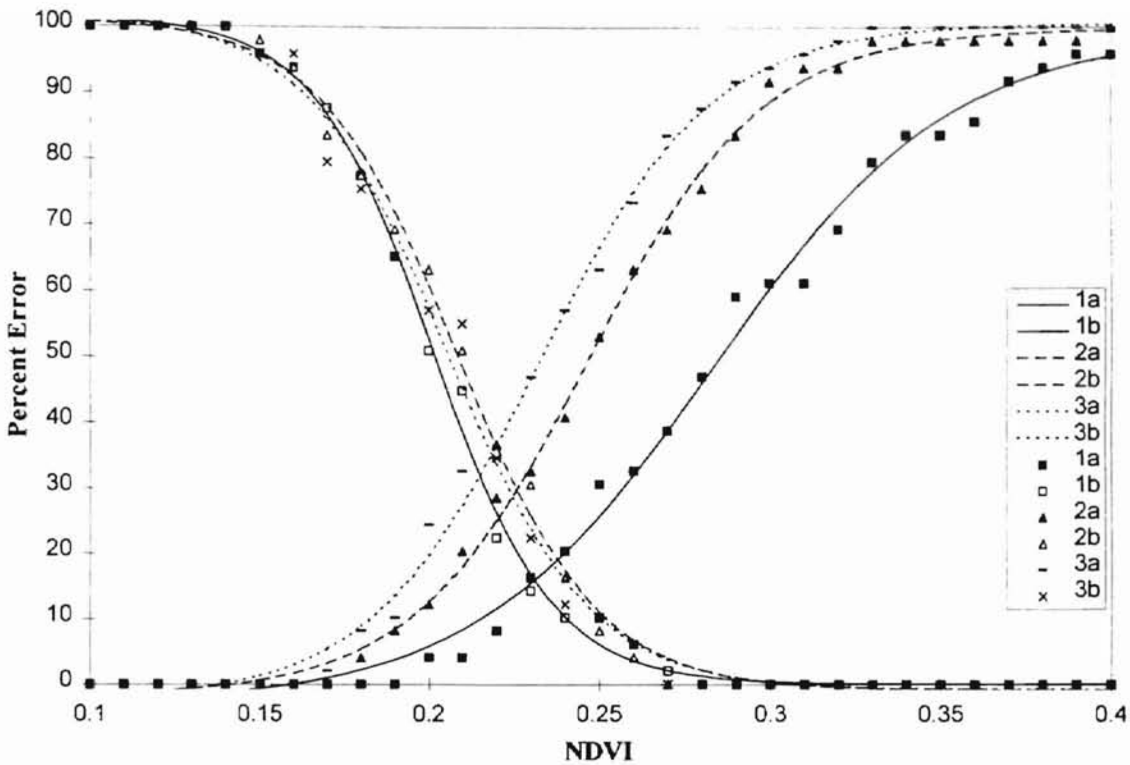

Figure 7--Errors vs. NDVI threshold from unpaired analysis. Error curves for 0.065, 0.129, and 0.194 m^2 fields-of-view

An economic study would be required to determine the optimum decision threshold for each image size and the allowable amount of each type of error. Such a study was beyond the scope of this paper. For the remainder of this study the optimum threshold was defined as the intersection of the two error curves. This value was used to describe the relationship of field-of-view size to error.

For unpaired data, as image size increased, it became increasingly difficult to distinguish between bindweed and soil images. Threshold error increased from 16.0% for an image size of 0.065 m^2 to 45.0% for an image size of 0.710 m^2. NDVI threshold decreased with increasing image size.

When the data set was separated by soil surface moisture, the threshold error was decreased for both the dry and moist subsets (fig. 8). The most noticeable decrease was in the moist soil subset. The trend of increasing error and decreasing threshold as image size increased was apparent in both subsets, as in the whole set analysis (table 3). Additionally, all of the threshold NDVI values for dry soils were lower than any of the moist soil NDVI thresholds.

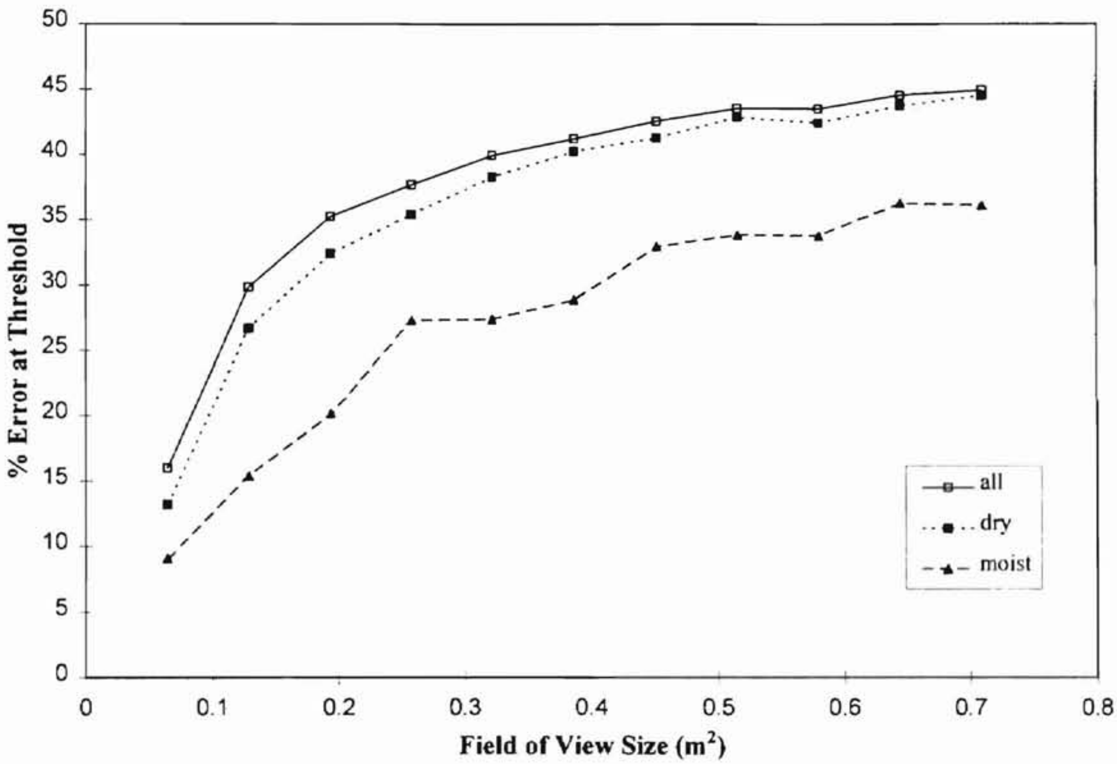

Figure 8--Threshold error vs. field-of-view size for unpaired analysis and classification by apparent soil moisture

Table 3. NDVI threshold and threshold error for all unpaired analysis

Image Area	Weed Cover*	Threshold Error (%)			NDVI Threshold		
(m^2)	(% field-of-view)	all	dry	moist	all	dry	moist
0.065	6.0	16.0	13.2	9.1	0.231	0.210	0.258
0.129	3.0	29.8	26.7	15.4	0.226	0.205	0.247
0.194	2.0	35.3	32.4	20.2	0.219	0.198	0.241
0.258	1.5	37.7	35.4	27.3	0.216	0.196	0.240
0.323	1.2	40.0	38.3	27.4	0.214	0.194	0.238
0.387	1.0	41.2	40.3	28.9	0.214	0.193	0.238
0.452	0.9	42.6	41.3	33.0	0.212	0.191	0.237
0.516	0.8	43.6	42.9	33.9	0.212	0.191	0.236
0.581	0.7	43.5	42.4	33.8	0.211	0.190	0.236
0.645	0.6	44.6	43.8	36.3	0.211	0.190	0.235
0.710	0.5	45.0	44.6	36.2	0.210	0.190	0.235

* Calculated from average bindweed size of 3900 mm^2

The paired t-test defined image size using adaptive thresholding. Soil variability between transects was accounted for by pairing and the detection threshold was appropriately adjusted. The unpaired analysis represented a sensing approach in which neither variability between plants or variability in background were accounted for, rather a spray or don't spray decision was based on a predetermined threshold. The former strategy allowed greater image sizes, but would be more difficult to implement. The latter would be easier to implement, but required a smaller field-of-view. The binary classification by moisture appearance was a compromise between the two strategies, and yielded results between the two Classification into more and better defined classes can be expected to produce results more comparable with the paired analysis.

Conclusions

It was possible to distinguish between images containing a single target bindweed on a soil background from images of the same soil without the bindweed for all field-of-view sizes tested. When soil and bindweed images were paired, detection success was 100% for nine out of the 11 fields-of-view tested and 98% for the other two.

At small fields-of-view, the bindweed-inclusive image response and the soil image response were easily distinguished, because the bindweed occupied a significant portion of the image. As the field-of-view increased, the difference between the responses diminished.

It was possible to detect bindweed with a single thresholding with considerable error at small image sizes. As image size increased, error also increased. In an unpaired analysis, error increased most dramatically, from 16.0 to 29.8%, between fields-of-view of $0.065 m^2$ and $0.129 m^2$.

Soil moisture was a significant factor in NDVI variability. Error was decreased by a binary classification based on the apparent presence of soil surface moisture. This indicated that visual classification of field conditions and appropriate threshold correction could reduce detection error and allow a larger field-of-view than no classification.

Field-of-view size and the detection system's ability to adjust for background variability are very much related. If the detection system can track and correct for changes in soil response, as demonstrated in the paired analysis, then field-of-view can be large and the possible error in detection will be small. However, if the detection strategy does not account for variation in soils, the possible error will be larger and the field-of-view size must be reduced.

Table 2. Error equation coefficients

Curve	Equation Coefficients all				dry				moist			
	A	B	C	D	A	B	C	D	A	B	C	D
0.065a*	-2.8322	101.9434	0.2829	0.0349	-3.2441	101.1265	0.2578	0.0289	-1.3398	97.9618	0.3150	0.0268
0.065b†	0.0606	101.3648	0.2015	-0.0176	-0.2085	100.9721	0.1862	-0.0129	0.3837	101.3332	0.2244	-0.0142
0.129a	-1.6681	101.4932	0.2464	0.0256	-2.3566	101.8706	0.2250	0.0214	-0.4910	98.3686	0.2738	0.0159
0.129b	-0.8347	102.0350	0.2087	-0.0204	0.1647	102.4354	0.1880	-0.0165	0.1901	100.4273	0.2322	-0.0088
0.194a	-2.3813	102.9261	0.2323	0.0250	-2.7207	101.9346	0.2100	0.0187	-0.8006	100.0178	0.2602	0.0143
0.194b	-0.7404	102.3839	0.2058	-0.0209	0.2511	103.1781	0.1846	-0.0168	0.7930	100.3046	0.2282	-0.0091
0.258a	-2.0980	102.6831	0.2266	0.0233	-2.4730	101.8978	0.2053	0.0176	-1.1117	100.8021	0.2531	0.0139
0.258b	-0.4879	102.2562	0.2055	-0.0203	0.2976	102.2023	0.1860	-0.0155	0.4157	100.8635	0.2288	-0.0111
0.323a	-1.8481	102.6352	0.2224	0.0227	-2.0423	101.6020	0.2007	0.0166	-0.8603	100.7367	0.2494	0.0121
0.323b	-0.7876	102.2035	0.2058	-0.0197	0.0942	102.5857	0.1857	-0.0154	0.1559	100.6690	0.2290	-0.0091
0.387a	-1.7599	102.7475	0.2211	0.0227	-2.6199	102.3222	0.1987	0.0172	-0.7378	100.7002	0.2478	0.0111
0.387b	-0.6786	102.0513	0.2066	-0.0196	0.1466	102.0152	0.1867	-0.0148	0.4128	100.4903	0.2299	-0.0088
0.452a	-1.8865	102.7122	0.2179	0.0221	-2.4900	102.2439	0.1960	0.0161	-1.0100	100.6549	0.2442	0.0109
0.452b	-0.7158	102.4838	0.2056	-0.0200	0.2682	102.0909	0.1856	-0.0144	0.1127	100.8593	0.2299	-0.0095
0.516a	-1.7708	102.7046	0.2168	0.0218	-2.8913	102.6561	0.1949	0.0166	-0.7111	100.5899	0.2427	0.0102
0.516b	-0.7391	102.2682	0.2063	-0.0200	0.2214	102.3642	0.1862	-0.0152	0.3245	100.4569	0.2297	-0.0092
0.581a	-1.9448	102.9057	0.2161	0.0221	-2.9012	102.7172	0.1940	0.0164	-0.6998	100.7800	0.2431	0.0107
0.581b	-0.7187	102.7029	0.2052	-0.0205	0.3312	102.2323	0.1849	-0.0148	0.3245	100.4569	0.2297	-0.0092
0.645a	-0.6483	101.2281	0.2152	0.0213	-2.8602	102.6192	0.1929	0.0164	-0.5797	100.6133	0.2412	0.0108
0.645b	-0.7670	102.5779	0.2059	-0.0205	0.2585	102.4351	0.1853	-0.0152	0.3798	100.3151	0.2302	-0.0088
0.710a	-2.0361	103.0137	0.2140	0.0220	-2.7461	102.3497	0.1920	0.0158	-0.5249	100.4834	0.2406	0.0095
0.710b	-0.7084	102.4449	0.2058	-0.0201	0.2216	102.0936	0.1857	-0.0146	0.4012	100.2924	0.2302	-0.0088

* Curve numbers ending in *a* are error in failing to detect bindweed

† Curve numbers ending in *b* are error in falsely detecting soil

References

Baret, F. and G. Guyot. 1991. Potentials and limits of vegetation indices for LAI and APAR assessment. *Remote Sensing the Environment* 35:161-173.

Beck, J. 1996. Reduced herbicide usage in perennial crops, row crops, fallow land and non-agricultural applications using optoelectronic detection. SAE Paper No. 96-1758. Warremdale, PA.: SAE.

Criner, B. R. 1998. Unpublished data.

Deering, D. W., J. W. Rouse, R. H. Haas, and J. A. Schell. 1975. Measuring :forage production" of grazing units from Landsat MSS data. In *Proceedings of the 10th International Symposium on Remote Sensing of Environment, II,* 1169-1178.

Felton, W. L., A. F. Doss, P. G. Nash and K. R. McCloy. 1991. A microprocessor controlled technology to selectively spot spray weeds. In *Proc. Automated Agricultural for the 21st Century Symposium*, 427-432. Chicago, IL.

"Field bindweed, *Convolvulus arvensis*". *Utah State University Extension noxious weeds list*. <//ext.usu.edu/ag/weeds/fbind.htm> (Jan. 1998).

Field bindweed official control program. 1988. K.A.R. 4-8-29. Topeka, KS: Kansas Department of Agriculture.

Huete, A.R. 1988. A soil-adjusted vegetation index(SAVI). *Remote Sensing of Environment* 25:295-309.

LandMaster BW label, Monsanto 1997 Crop Chemical and MSDS Book, 1997. Pages 163-167.

Lillesand, T. M. and R. W. Kiefer. 1994. *Remote Sensing and Image Interpretation.*

New York: John Wiley & Sons, Inc.

Majek, B. A. 1993 Bindweed identification and control. FS676. New Brunswick, NJ.: Rutgers Cooperative Extension.

Merritt, S. J., G. E. Meyer, K. Von Bargen, and D. A. Mortensen. 1994. Reflectance sensor and control system for spot spraying. ASAE paper no. 94-1057. St. Joseph, MI.: ASAE.

Nitsch, B. B., K. Von Bargen, G. E. Meyer, and D. A. Mortensen. 1991. Visible and near-infrared plant, soil and crop residue reflectivity for weed sensor design. ASAE Paper No. 91-3006. St. Joseph, MI.: ASAE.

Richardson, A. J., C. L. Wiegand. 197. Distinguishing vegetation from soil background information. *Photogramnetric Engineering and Remote Sensing* 43(12):1541-1552.

Rouse, J. W. Jr., R. H. Haas, D. W. Deering, J. A. Schell, and J. C. Harlan. 1974. Monitoring the venal advancement and retrogradation (green wave effect) of natural vegetation. In *NASA/GSFC Type III Final Report*, 371. Greenbelt, MD.

Steel, R. G. D. and J. H. Torrie. 1980. *Principles and Procedures of Statistics: A Boimetrical Approach.* New York: McGraw-Hill, Inc.

Stone, M. L. 1994. Embedded neural networks in real time controls. SAE Paper No. 94-1067. Warrendale, PA.: SAE.

Stone, M. L., J. B. Solie, R. W. Whitney, W. R. Raun and H. L. Lees. 1996. Sensors for detection of nitrogen in winter wheat. SAE Paper No. 96-1757. Warrendale, PA.: SAE.

Zollinger, R. K. and R. G. Lym. 1996. Identification and control of field bindweed. W802. Fargo, ND: North Dakota State University Extension Service.

Chapter IV

Recommendations for Further Study

There is much work yet to be done to create a functional and efficient sensor/applicator for detection and control of bindweed. This study provided useful information and conclusions for the eventual development of a bindweed sensor, as well as developing methods for future work. This study established field-of-view size requirements for a sensor to detect bindweed under various environmental conditions, and developed relationships of field-of-view size to detection strategy, by examining variable, fixed, and classification thresholding.

Measurements during this study were collected in one field of one soil type. It should be determined if the results of this study are directly applicable to other soils and environmental conditions. Recommendations for further work include studies to determine how reflective properties and detection ability change with background soil type, with changing conditions in each soil type, and with the presence of crop residues in the background soils. Field-of-view requirements and detection ability in early morning and late evening when low light levels and low solar zenith angles are known difficulties should also be examined. Also, an economic study will be needed to determine the magnitude of errors that are acceptable in a control program.

It was a conclusion of this study that field-of-view size and the ability to adjust for background variability are very much related. When variations in background conditions was accounted for, detection ability improved and field-of-view requirements increased.

Also no single field-of-view or NDVI threshold could be successfully used for all conditions. Both of the these statements lead to the conclusion that to implement a reliable on-the-go bindweed detection sensor, some type of adjustable or adaptive threshold strategy is needed. Studies to determine spatial information about the magnitude and frequency of background variability, and the patterns and frequencies of bindweed infestations are also recommended.

Appendix

Visual Basic Programs Used in Chapters II and III

Spread Sheet format for Bindweed/Soil Image Size Simulation

	A	B	C	D	E	F	G	H	I	J	K	L
1												
2												
3	Bindsize	##		ImageSize	##		##		##		0	
4	in pixles				***compNDVI***	***soilNDVI***	***compNDVI***	***soilNDVI***	***compNDVI***	***soilNDVI***		
5	Error I	*0.##*			##	##	##	##	##	##		
6	(0-1)				##	##	##	##	##	##		
7					##	##	##	##	##	##		
8	Rbind mean	##			##	##	##	##	##	##		
9	Rbind stdev	##			##	##	##	##	##	##		
10	NIRbind mean	##			##	##	##	##	##	##		
11	NIRbind stdev	##			##	##	##	##	##	##		
12	Rsoil mean	##			##	##	##	##	##	##		
13	Rsoil stdev	##			##	##	##	##	##	##		
14	NIRsoil mean	##			##	##	##	##	##	##		
15	NIRsoil stdev	##			##	##	##	##	##	##		
16					##	##	##	##	##	##		
17	soil std. error	##			##	##	##	##	##	##		
18	bind std. error	##			##	##	##	##	##	##		
19	soil dev SSred	##			##	##	##	##	##	##		
20	bind dev SSred	##			##	##	##	##	##	##		
21	soil count	##										
22	bindweed count	##										
23	soil slope	##		red and nir regression equation must have the form:								
24	soil intercept	##		NIR = m*RED + b								
25	bind slope	##										
26	bind intercept	##										
.												
.												
54					##	##	##	##	##	##		
55					##	##	##	##	##	##		
.												
.												
74												
75		***ImageSize***		##	##	##	##				user input parameters	
76		***NDVI @error I***		##	##	##	##				computer generated	
77		***% error II***		*0.##*	*0.##*	*0.##*	*0.##*					
78												

Simulation Program Described in Chapter II

```
Sub bindsim()
'Bindweed/Soil Field of View Simulation
'Chapter II in Thesis
'Byron R. Criner  3/1/97
' updated 7/24/97  with if statments to check rnd function return for 0<f<1
' also added randomize function at the beginning of each image size loop
'   to seed random generator by computer clock
'

'Program to randomly sample a normal population of composite bindweed and soil NDVIs
'and compare to all soil NDVI for same sample size.  This comparison can be done for
'any minimum size of bindweed and any image size from one pixle up.

'User must input:   Minimum Target Bindweed Size (in no. of pixles)
'              Image Sizes to Sample (in no. of pixles)
'              Acceptable error of not spraying bindweed (Error I as a decimal)
'              Mean and Stdev. for soil and bindweed RED and NIR samples
'Output will be:   ImageSize(in no. of pixles)
'              Threshold NDVI
'              % error of spraying bare soil
'One pixle size is a 2" diameter circle.  Area = 3.1415 in^2
'format for activeSheet.Cells(row, colum).Value

meanA = ActiveSheet.Cells(12, 2).Value   'Get mean of REDsoil pop. from a cell
meanB = ActiveSheet.Cells(14, 2).Value   'Get mean of NIRsoil pop. from a cell
stdA = ActiveSheet.Cells(13, 2).Value    'Get stdev. of REDsoil pop. from a cell
stdB = ActiveSheet.Cells(15, 2).Value    'Get stdev. of NIRsoil pop. from a cell
meanC = ActiveSheet.Cells(8, 2).Value    'Get mean of REDbindweed pop. from a cell
meanD = ActiveSheet.Cells(10, 2).Value   'Get mean of NIRbindweed pop. from a cell
stdC = ActiveSheet.Cells(9, 2).Value     'Get stdev. of REDbindweed pop. from a cell
stdD = ActiveSheet.Cells(11, 2).Value    'Get stdev. of NIRbindweed pop. from a cell
soilstderror = ActiveSheet.Cells(17, 2).Value 'Get soil std. error from a cell
bindstderror = ActiveSheet.Cells(18, 2).Value 'get bindweed std. error from a cell
soilSSred = ActiveSheet.Cells(19, 2).Value   'get dev. SSred for soil from cell
bindSSred = ActiveSheet.Cells(20, 2).Value   'get dev. SSred for bindweed from cell
soilcount = ActiveSheet.Cells(21, 2).Value   'gets number of true soils imaged from a cell
bindcount = ActiveSheet.Cells(22, 2).Value   'gets number of true bindweed images from a cell
soilslope = ActiveSheet.Cells(23, 2).Value   'gets soil slope for nir/r regression equation
soilintercept = ActiveSheet.Cells(24, 2).Value 'gets intercept for nir/r regression equation
bindslope = ActiveSheet.Cells(25, 2).Value
bindintercept = ActiveSheet.Cells(26, 2).Value

cntimage = 5   'counts images
cnt2 = 5       'counts images in output

Do While ActiveSheet.Cells(3, cntimage).Value <> 0       'end loop with a zero
  'loop will generate ndvi readings and output for each image size in spreadsheet
 imagesize = ActiveSheet.Cells(3, cntimage).Value      'get imagesize from sheet
 bindsize = ActiveSheet.Cells(3, 2).Value              'Get BindSize from a stationary cell
```

```
' check to see if imagesize is as large as target bindweed
If imagesize <= bindsize Then
   bindsize = imagesize
End If

dirtsize = imagesize - bindsize          'define dirtsize
ActiveSheet.Cells(4, cntimage).Value = "compNDVI"
ActiveSheet.Cells(4, cntimage + 1).Value = "soilNDVI"

For l = 6 To 105        'calculate 100 reps of NDVI for each image size

Randomize

  ' ******** COMPUTE COMPOSITE NDVI ******
  A = 0   ' Pop RED Soil
  B = 0   ' Pop NIR Soil
  C = 0   ' Pop RED Bindweed
  D = 0   ' Pop NIR Bindweed
  For i = 1 To dirtsize        ' DirtSize is # of dirt pixles in an image
     f = Rnd()            ' generate a random frequency between 0 and 1
     If f = 0 Then f = 0.00001
     If f = 1 Then f = 0.99999
     red = Application.NormInv(f, meanA, stdA)   'finds a red based on f
     A = red + A                        'adds all soil reds in image
     stdNIR = (soilstderror ^ 2 * ((1 / soilcount) + ((red - meanA) ^ 2 / soilSSred))) ^ 0.5
     nir = (soilslope * red) + soilintercept      'regression equation
     f2 = Rnd()
     If f2 = 0 Then f = 0.0001
     If f2 = 1 Then f = 0.9999
     nir2 = Application.NormInv(f2, nir, stdNIR)
     B = nir2 + B
  Next i

  For j = 1 To bindsize        ' BindSize is # of bindweed pixles in an image
     f = Rnd()            ' generate a random frequency between 0 and 1
     If f = 0 Then f = 0.0001
     If f = 1 Then f = 0.9999
     red = Application.NormInv(f, meanC, stdC)
     C = red + C
     stdNIR = (bindstderror ^ 2 * ((1 / bindcount) + ((red - meanC) ^ 2 / bindSSred))) ^ 0.5
     nir = (bindslope * red) + bindintercept
     f2 = Rnd()
     If f2 = 0 Then f2 = 0.0001
     If f2 = 1 Then f2 = 0.9999
     nir2 = Application.NormInv(f2, nir, stdNIR)
     D = nir2 + D
  Next j

  compNDVI = ((D + B) - (A + C)) / (A + B + C + D)     'composite NDVI
  ActiveSheet.Cells(l, cntimage).Value = compNDVI

  ' ********** COMPUTE SOIL NDVI ********************
  A = 0  ' reset Pop RED Soil
  B = 0  ' reset Pop NIR Soil
```

```
  For k = 0 To imagesize    ' DirtSize is # of dirt pixles in an image
     f = Rnd()              ' generate a random frequency between 0 and 1
     If f = 0 Then f = 0.0001
     If f = 1 Then f = 0.9999
     red = Application.NormInv(f, meanA, stdA)    'finds a red based on f
     A = red + A                              'adds all soil reds in image
     stdNIR = (soilstderror ^ 2 * ((1 / soilcount) + ((red - meanA) ^ 2 / soilSSred))) ^ 0.5
     nir = (soilslope * red) + soilintercept      'regression equation
     f2 = Rnd()
     If f2 = 0 Then f2 = 0.0001
     If f2 = 1 Then f2 = 0.9999
     nir2 = Application.NormInv(f2, nir, stdNIR)
     B = nir2 + B
   Next k

  soilNDVI = (B - A) / (B + A)              'soil NDVI
  ActiveSheet.Cells(l, cntimage + 1).Value = soilNDVI
 Next l     'End 50 replications loop


' *************** mean and stdev ******************



' ********* generate output portion of spreadsheet at row 75 ********

ActiveSheet.Cells(110, cnt2).Value = ActiveSheet.Cells(3, cntimage) 'imagesize output

q = ActiveSheet.Cells(5, 2).Value                        'q from a cell
        'q is the percent (0-1) of allowable error in missing bindweed
        'If 90% of the bindweed was the target, then the allowable error would be q = .1
mean = Application.Average(Range(Cells(6, cntimage), Cells(105, cntimage)))
std = Application.StDev(Range(Cells(6, cntimage), Cells(105, cntimage)))
x = Application.NormInv(q, mean, std)
        'returns a NDVI value corresponding to q
ActiveSheet.Cells(111, cnt2).Value = x  '111 should be 76                'Threshold output

ActiveSheet.Cells(107, cntimage).Value = mean
ActiveSheet.Cells(108, cntimage).Value = std



 mean = Application.Average(Range(Cells(6, cntimage + 1), Cells(105, cntimage + 1)))
std = Application.StDev(Range(Cells(6, cntimage + 1), Cells(105, cntimage + 1)))
ActiveSheet.Cells(107, cntimage + 1).Value = mean
ActiveSheet.Cells(108, cntimage + 1).Value = std



f = Application.NormDist(x, mean, std, True)
If Not IsNumeric(f) Then  ' check for valid number
    f = 1
 End If
```

```
  y = 1 - f
        'percentile of soilNDVI population @ x NDVI value
        'y is the percent error of sensing bare dirt as bindweed
 ActiveSheet.Cells(112, cnt2).Value = y  '112 should be 77          'Error II output

 cnt2 = cnt2 + 1         'counts colums for output of spreadsheet
 cntimage = cntimage + 2

Loop  'ends {do while there is an image size} loop
    'image size loop ends when image size value in row 2 = 0

'Label output
ActiveSheet.Cells(110, 3).Value = "Image Size"
ActiveSheet.Cells(111, 3).Value = "NDVI at Error I"
ActiveSheet.Cells(112, 3).Value = "% Error spray soil"

 End Sub
```

Program for Creating Fields-of-view and calculating NDVI from Chapter III

```
' threshold_test Macro
' Macro recorded 11/12/97 by criner

Sub threshold_test()
' prepared for 49 samples and 11 different image sizes
' calculates % error in missing bindweed and falsly spraying soil for thresholds between -.5 and 1
' Y1 = bindweed
' Y2 = soil
ActiveSheet.Cells(1, 32).Value = "Threshold Error Test"
z = 32
q = 34
For k = 1 To 11 ' image size loop
  y1 = 0
  y2 = 0
  threshold = 0
  x = 7
  Do While threshold < 0.5
    i = k + 6
    soil_error_count = 0
    bind_error_count = 0
    For j = 1 To 29 'number of samples loop
      y1 = ActiveSheet.Cells(i, 21).Value
      'ActiveSheet.Cells(j, q).Value = y1
      y2 = ActiveSheet.Cells(i, 22).Value
      'ActiveSheet.Cells(j, (q + 1)).Value = y2
      If y2 > threshold Then
        soil_error_count = soil_error_count + 1
      End If
      If y1 < threshold Then
        bind_error_count = bind_error_count + 1
      End If
      i = i + 13
    Next j
    q = q + 2
    soil_error = 100 * (soil_error_count / 29)
    bind_error = 100 * (bind_error_count / 29)
    ActiveSheet.Cells(x, z).Value = bind_error
    ActiveSheet.Cells(x, (z + 1)).Value = soil_error
    ActiveSheet.Cells(x, 31).Value = threshold
    threshold = threshold + 0.01
    x = x + 1 ' x is dictated by the number of thresholds tried
  Loop   'ends while threshold < 1 loop
  ActiveSheet.Cells(6, z).Value = "bind error"
  ActiveSheet.Cells(6, (z + 1)).Value = "soil error"
  area = k * 100
  ActiveSheet.Cells(4, z).Value = "area = "
  ActiveSheet.Cells(4, (z + 1)).Value = area
  z = z + 2 ' move over two to start a new error set for increased image size
```

```
Next k
End Sub
```

2

VITA

Byron Ray Criner

Candidate for the Degree of

Master of Science

Thesis: FIELD-OF-VIEW DETERMINATION FOR A BINDWEED DETECTION SENSOR

Major Field: Biosystems Engineering

Biographical:

Personal Data: Born in Tulsa, Oklahoma on November 30, 1970, the son of Raymond T., Jr. and Linda A. Criner.

Education: Graduated from Haskell High School, Haskell, Oklahoma in May, 1989; received a Bachelor of Science degree in Agricultural Engineering from Oklahoma State University, Stillwater, Oklahoma in May, 1994. Completed the requirements for the Master of Science degree with a major in Biosystems Engineering from Oklahoma State University in May, 1998.

Professional Experience: Raised on a cattle and wheat farm near Haskell, Oklahoma, employed as a farm laborer; employed by Oklahoma State University, Department of Biosystems and Agricultural Engineering as an undergraduate engineer assistant and a research engineer.

Professional Memberships: Oklahoma State Board of Registration for Professional Engineers and Land Surveyors certified Engineer Intern, American Society of Agricultural Engineers Student Branch.